NTNU – Trondheim
Norwegian University of
Science and Technology

Radiation fields and viscous cosmology

Friction in General Relativity

Tobias Grøsfjeld

MSc in Physics
Submission date: May 2015
Supervisor: Kåre Olaussen, IFY

Norwegian University of Science and Technology
Department of Physics

Radiation fields and viscous cosmology

Tobias Grøsfjeld

May 15, 2015

Abstract

Certain aspects of the Lorentz transformation, sometimes called beaming, aberration or transverse Doppler effect, induce viscosity-like effects on extended objects moving through radiation fields. In this thesis, these effects are investigated in the contexts of a cosmic background radiation and near a Schwarzschild star.

Sammendrag

Visse aspekter ved Lorentztransformasjonen, noen ganger kalt beaming, aberrasjon eller transversal Doppler-effekt, fører til viskositetslignende effekter på utstrakte objekter som beveger seg gjennom strålingsfelt. I denne oppgaven undersøkes disse effektene for kosmisk bakgrunnstråling og i nærheten av en Schwarzschild-stjerne.

Preface

This thesis is the result of a personal initiative by the author, rather than being a project presented by the faculty as master's material. As a consequence, the initial formulation of the problem was somewhat more vague than your average NTNU thesis, and it took an entire year to discover century-old material on related subjects such as the YORP or Poynting-Robertson effects. With such intuitive names, I obviously should have guessed.

The work has mostly been independent, with the exception of some article exchanges and email correspondence with my advisor, professor Kåre Olaussen, who reviewed the final product. He also held the course on gravity and cosmology I attended in my BSc, and it was while working on his problem sets on relativistic beaming that the idea of a viscous metric first entered my head. This inspired me to investigate relativistic fluid mechanics and wonder about non-conservative systems.

Notation

This document uses a $(+---)$ metric and $c = 1$ units unless otherwise noted. Equations are not necessarily simplified by hand, but by the Maple software.

Contents

1 Introduction **1**
- 1.1 Aberration of light . . . 2
- 1.2 The Poynting-Robertson effect . . . 3
- 1.3 Thermal effects and rotating bodies . . . 6

2 General relativistic dynamics **9**
- 2.1 A little differential topology . . . 9
- 2.2 The variational principle . . . 11
- 2.3 Curved lines in curved space . . . 12
- 2.4 Rotation and torques . . . 14

3 The Stress-Energy Tensor **17**
- 3.1 The Poynting-Robertson effect revisited . . . 19
- 3.2 The Einstein field equations . . . 21

4 Near a Schwarzschild star **23**
- 4.1 Effective cross-sections . . . 25
- 4.2 Radiation pressure in the Solar system . . . 28

5 The cosmic background fluid **31**
- 5.1 Relativistic fluids . . . 32
- 5.2 A model of shadow . . . 34

6 Conclusion and considerations **39**

Chapter 1

Introduction

In introductory physics one learns to think in terms of mechanical vectors and scalars, and a common problem posits a schematic description of a physical configuration, challenging the student to intuit which physical laws to use and which equations to write down.

As one transitions to a general relativistic mindset, one may find that the ways to answer intuitive questions become more opaque. Since the classical force of gravity is purely attractive, every kinematic impact or collision that overcomes the pull of gravity must include something more. As amusing as it sounds, it would take an insane model to see yourself in a mirror and conclude that every photon was reflected through gravitational lensing. However, including these additional interactions can be challenging, as formal rigor must take priority over intuition once vectors become local and tensors too complex to visualize.

A prime example is the damped harmonic oscillator experiencing viscosity. Whereas one in Lagrangian mechanics could include non-conservative friction terms through the Rayleigh dissipation function, how does one implement such an effect in a relativistic capacity? It is important that energy-momentum is locally conserved, so any such dissipation must be kept track of if it is to later generate the curvature of space-time, but how?

We know from the special theory of relativity that the observed passage of time and space can change with one's reference frame, but can the metric itself be viscous? From a mathematical point of view such a proposition sounds strange, but if curvature can be an emulation of position-dependent acceleration, it's far from obvious that it would not also be capable of emulating velocity-dependent acceleration once the metric is a dynamic variable.

As one ponders these questions, one is invariably reminded of the concept of the aether. Though it has long since been dismissed as a velocity-governing medium for light, the Doppler effect implies that the cosmic background radiation still provides an ever-so-slight velocity-dependent radiation pressure on a moving observer, so any complete cosmological model would need to treat its "viscosity" - or rather, the energy loss of any moving observer to the anisotropic ambient radiation field.

By the same token, as the Earth orbits the Sun it moves through a radiation field, which should slow down the orbit through collisions with the photons from the side. Evidently, the Earth's been orbiting for a long time and looks to keep orbiting for quite a while longer, so why does this seem to not be happening?

The fluid dynamics treated in introductory courses on general relativity tend to restrict it to perfect fluids - ones that are isotropic, homogeneous and free of viscosity - and these are primarily used to derive the FRW cosmological models rather than for any local treatment.

This thesis, however, asks the question of how to treat the general kinematics of local interaction with relativistic fluids, and primarily considers two interesting special cases: interaction with the cosmic background radiation, and movement through the radiation field around a Schwarzschild star. On the way, we seek to understand how these viscosity-like effects relate to the curvature of space-time, if at all.

The text is set up to highlight the transition from the classical mindset to the relativistic one, by first treating a motivating and intuitive special relativistic effect in chapter 1, then introducing the language of general relativity in chapter 2 and 3, and finally analyzing the viscosity-like effects and their relation to curved geometry in the chapter 4 and 5.

1.1 Aberration of light

We start off in the context of special relativity by attempting to establish an intuition for how the Lorentz transform affects radiation, hopefully highlighting some physical implications.

"Aberration" refers to how the Lorentz transform can bend beams of light. A characteristic example of aberration can be visualized by considering an isotropically radiating object in its rest frame versus a frame where it is moving.

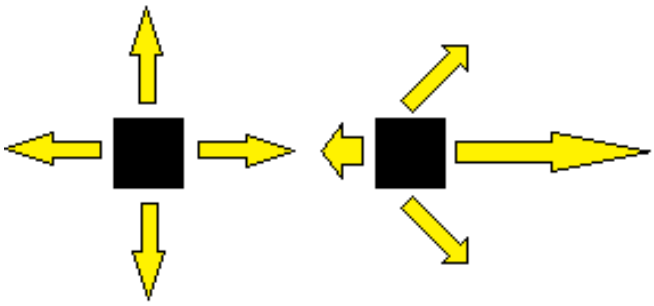

Figure 1.1: Intensities in the rest frame (left) and moving frame (right).

In the rest-frame, the forces on the object caused by the departing photons cancel thanks to the isotropy, so it remains at rest. However, in the moving frame the departing photons are Doppler-shifted, so they must be more energetic in the forward direction. The radiation is now anisotropic, and according to Newton's third law there is an apparent net force opposite the direction of motion. This is seemingly paradoxical; does the object accelerate or not?

Thankfully, the paradox can be explained in the covariant formalism using four-momenta: Even in the rest frame there is a momentum change $\dot{p}^\mu$, but it arises from the object losing *energy* to the radiation:

$$\dot{p}^\mu = (-\Phi, \mathbf{0}) \qquad \text{(Rest frame)} \tag{1.1a}$$

$$\dot{p}^\nu = \Lambda^\nu_\mu \dot{p}^\mu = (-\gamma\Phi, -\gamma\Phi\vec{\mathbf{v}}) \qquad \text{(Moving frame)} \tag{1.1b}$$

which effectively means it is getting *lighter* (less massive), not slower.

1.2 The Poynting-Robertson effect

The Poynting-Robertson effect describes the effect of aberration on a black body moving in an approximately circular orbit around a star. As with many effects in relativity there are several ways to visualize it depending on choice of reference frame. One way is to think of it as a variant of the aberrant force from the previous section where the energy is constantly being refilled by the nearby star, leaving only the accelerative force. Another way is to imagine it in the object's co-moving frame as similar to running through a rain of radiation.

The rain-running analogy[1]

Imagine there is no wind on a rainy day. An observer standing still will see the rain as falling straight down, but a moving one will start crashing into droplets from the side. From their reference frame it looks like the rain is falling at an angle, as if there was wind.

When it comes to the vertical component of the rain, things are pretty much the same - whenever they move out of the path of one droplet, they move into the path of another, so the big difference is the added horizontal component of the rain. The faster the observer runs, the faster they get wet, and even if there was no air resistance, the water would provide resistance of its own through momentum transfer to the observer.

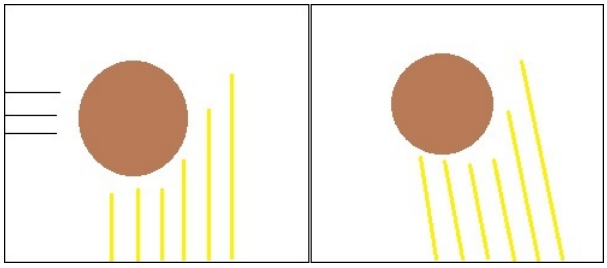

Figure 1.2: Radiation in the stellar frame (left) and planet frame (right).

Objects moving through space can experience something similar. While there is no inherent aether-resistance for the movement of planets to emulate wind resistance, space is not a perfect vacuum. Planets are constantly bombarded by radiation, and near a star it plays the part of the rain in the above analogy: The faster your orbit, the more radiation pressure seems from come from the front, slowing you down. It's important to note that this is separate from the electric field rotating into a magnetic field under a Lorentz transformation; in the radiation domain this is a purely kinetic effect.

Since planet orbits seem to be stable we can intuit that this effect must be very weak and certainly dominated by gravity on the macroscopic scale. However, if the parameters are just right this velocity-dependent force could have a significant impact on a trajectory.

[1] MinutePhysics has an excellent short video on running through the rain on their Youtube channel, which can be found at http://www.youtube.com/watch?v=3MqYE2UuN24

Calculation of the Poynting-Robertson effect

What is now known as the Poynting-Robertson effect was first predicted by J.H. Poynting[3] in 1903 using the then-popular context of a luminiferous aether, who calculated it to be

$$F_{PR} = vWA \tag{1.2}$$

where v is the orbital speed of the object in the stellar rest frame and W is the incoming radiation power flux on its cross-section A. In 1937 this result was verified by Robertson[4] in the context of general relativity.

To simplify calculations, we consider a locally Minkowski coordinate system (t, x, y, z) far away from the source of radiation and aligned such that in the stellar frame, the photon momenta are all given along the tangent vector $\lambda^\mu = (1, 1, 0, 0)$ with energy density W, and the particle's 4-velocity is given by $u^\mu = (\dot{t}, \dot{x}, \dot{y}, \dot{z}) = (\gamma, 0, \gamma v, 0)$.

If we once more model the object as a black body which radiates its thermal energy isotropically, its momentum change is the momentum of absorbed photons per unit of time. We will calculate the effect for two kinds of object: Firstly a sphere, which has the computational benefit of the cross-section in the rest frame being the same no matter the angle of incoming photons, and secondly a cube, which highlights the physics of how different kinds of surface element move through radiation.

Sphere

For a black sphere with cross-sectional area A, the force experienced in the sphere's rest frame is given by the momentum flux onto A. The photon density Lorentz-contracts[2] to γW and the direction is simply given along the λ-vectors transformed to the sphere's rest frame, resulting in a force of

$$F^\mu_{\text{Sphere}} = \begin{cases} (0, & \gamma, -\gamma^2 v, 0)WA & \textbf{(Rest frame)} \\ (-\gamma^3 v^2, & \gamma, -\gamma^3 v, 0)WA & \textbf{(Stellar frame)} \end{cases} \tag{1.3}$$

where we have assumed the absorbed energy in the rest frame is immediately re-emitted isotropically, counterbalancing the time-indexed component of $\dot{p}$.

Cube

For a black cube with side areas A aligned along its trajectory, the four-force can split into the two contributions coming from the front surface and the side surface. The frontal momentum per eigentime is given analogously to the rain-running analogy by

$$\begin{aligned} \text{Force}_{\text{Front}} &= \left(\frac{\text{Momentum}}{\text{photon}}\right) \times \left(\frac{\text{Photons}}{\text{time}}\right) \\ &= \left(\frac{\text{Momentum}}{\text{photon}}\right) \times \frac{\text{Photons}}{\text{Volume}} \times \left(\text{Area} \times \frac{\text{Distance}}{\text{time}}\right) \qquad (1.4) \\ \Rightarrow F^\mu_{\text{Front}}(v) &= \Lambda^\mu_\sigma(-v)(0, 1, -\gamma v, 0)^\sigma WA\gamma v \qquad (1.5) \\ &= (-\gamma^3 v^3, \gamma v, -\gamma^3 v^2, 0)WA \end{aligned}$$

[2] Guess treats a spherical source in his paper[2] and arrives at the same result.

We see the collision force in the y direction is $\propto \gamma^3 v^2 W$, which is intuitive in the sense that you collide with "faster" particles at a faster rate. However, there's also an apparent *drag* on the surface in the x direction! It's noteworthy that if the surface had been reflective instead of black, that drag would not have occurred - even if it were to rotate so a surface pointed directly toward the radiation, a reflective surface would experience a force more similar to the black sphere than the black cube.

For the side-surface we don't need the velocity or volume term, because whenever you move out of the way of one photon you move into the path of another. In the rest frame, the relativistic correction arising from the Lorentz-contracted number density balances against the time-dilated collision rate, owing to the fact that the speed of light is constant and proportionally less of it is going sideways.

$$F^{\mu}_{\text{Side}} = W(-\gamma^2 v^2, 1, -\gamma^2 v, 0) \tag{1.6}$$

totaling

$$F^{\mu}_{\text{Tot}} = (1+\gamma v) W(-\gamma^2 v^2, 1, -\gamma^2 v, 0) \tag{1.7}$$

We see that the proportionality between the cube and the sphere is $\frac{1+\gamma v}{\gamma}$, which corresponds to how the cube's cross-section is increased at high speeds due to the inclination of the radiation in the rest frame.

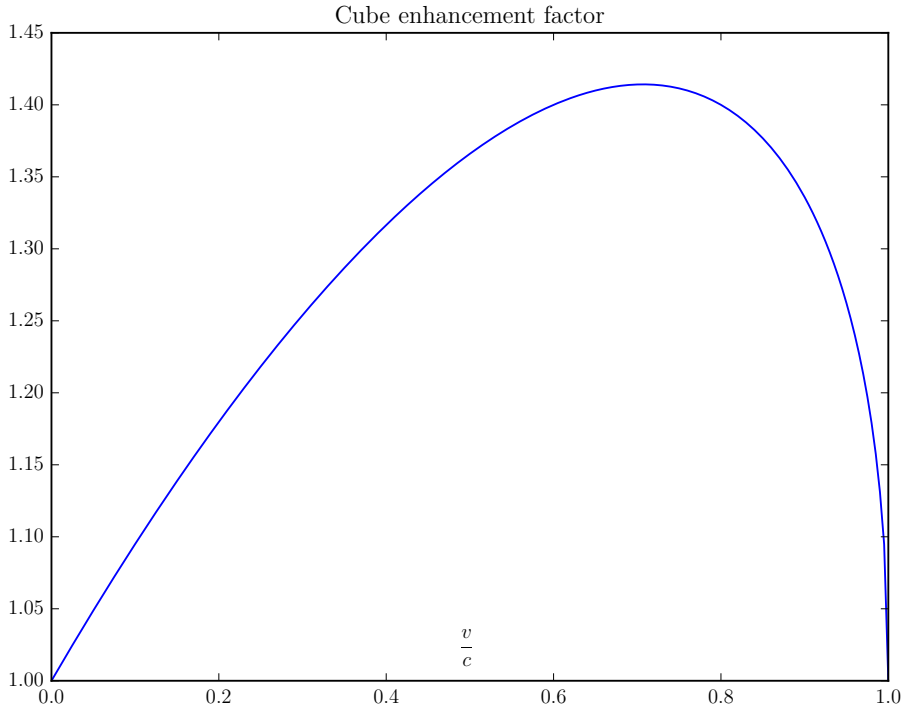

Figure 1.3: The increase in cross-section for a moving cube. One could say that this makes the sphere more "photo-dynamic" than the cube.

Observed 3-acceleration

The 4-acceleration is related to the observed 3-acceleration by

$$\vec{F}/m = \partial_\tau \vec{U} = \partial_\tau(\gamma\vec{v}) = \dot{\gamma}\vec{v} + \gamma\vec{a} = \gamma^3(\vec{v}\cdot\vec{a})\vec{v} + \gamma\vec{a} = \gamma^3\vec{a}_\parallel + \gamma\vec{a}_\perp \tag{1.8}$$

where we used $(1+\gamma^2v^2)\vec{a}_\parallel = \gamma^2\vec{a}_\parallel$ to decompose $\vec{a}$ into parallel and orthogonal components. If we disregard the transverse component for a sphere, we can now write down a simple differential equation governing the evolution of the orbital velocity v in the stellar frame in terms of eigentime

$$\partial_\tau v = -\frac{vWA}{m} \Rightarrow v(\tau) = v(0)e^{-\frac{WA}{m}\tau} \tag{1.9}$$

which agrees with Poynting and Robertson's results.

Here we observe the effective "viscosity" of light at work, as it is damped similarly to the amplitude of the damped harmonic oscillator. Once we have introduced some necessary tools, we will revisit the Poynting-Robertson effect in more detail in chapter 3.

1.3 Thermal effects and rotating bodies

In the previous section, the cube happened to have equal drag forces on each surface, so if we assume the center of mass to be in the center of the cube, it experienced no net torque. Furthermore, it was assumed perfectly conductive and did not accrue inertia from being heated.

These assumptions may yield good approximations for small objects, but since the speed of heat diffusion is only material dependent we can expect large objects to be able to radiate anisotropically[5]. Even highly conductive bodies that do radiate isotropically can experience a torque owing to the stress on its surfaces relative to the center of energy. These thermal effects are usually weak, but can have long-term consequences for orbits, rotations and precession. For instance, Asteroid 2009FD may or may not be on a collision course with Earth around 2190[6], and that time scale is sufficiently long for higher-order thermal phenomena like the Yarkovsky effect to be relevant.

Orbital effects

Diurnal pressure means that the warmer day-side emits more than the cold night-side, partially bridging the gap between the radial force experienced by black and reflective bodies in orbit. (See eq. (4.9) and eq. (4.8))

The diurnal Yarkovsky effect occurs on a rotating body due to day/night-cycles. The absorbed heat is not instantly emitted, and so the areas in dusk are warmer than the areas in dawn, which can speed up or slow down the orbit depending on the direction of rotation.

The seasonal Yarkovsky effect occurs on orbiting bodies. Areas in fall are warmer than areas in spring, slowing down orbital speed. This effect is more significant for an object precessing on a tilted axis.

Rotational effects

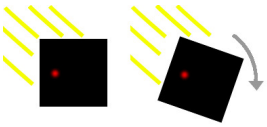

Buoyancy can be intuited as similar to how parachutes or sailboats align with the direction of air-flow, thereby defining an "up".

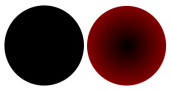

Inertial amplification occurs to rotating bodies and black bodies, as the energies near the surface are higher than near the center of rotation, thus contributing slightly more to the inertia. Realistically, most materials will tear themselves apart before this becomes relevant.

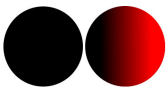

Inertial shift occurs when the center of energy shifts due to the thermal energy distribution. It's an extremely weak effect, and can only affect large, slowly-rotating black bodies with very low density to any measurable degree.

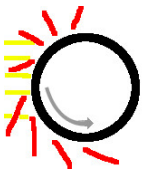

Rotational beaming occurs to rapidly rotating black bodies. Incoming radiation drags more on the dawning side than the dusk side, slowing down the rotation. Warm bodies emit photons at an angle, causing an apparent torque even if the rest frame has none. However, if there are no other causes of torque the situation is much like linear aberration: no angular acceleration is realized, for the decrease in angular momentum comes instead from the reduced moment of inertia. This can be thought of as the Poynting-Robertson effect of rotation.

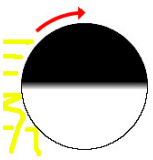

The YORP albedo effect occurs on an object with variations in albedo.[3] Among thermodynamic considerations, darker areas are dragged, reflective areas are not, so a half-black, half-white sphere would begin rotating its black hemisphere toward night-time.

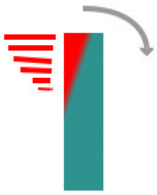

The thermal YORP effect describes rotational emission pressure, i.e. when the temperature distribution is such as to cause a torque. Affects, for instance, an impact crater on a hillside.

While each of these effects have their domain of relevance, we will in this document mostly restrict ourselves to modelling symmetric, non-rotating and perfectly conductive objects, for which only the Poynting-Robertson effect is a primary concern.

[3] "YORP" referring to Yarkovsky-O'Keefe-Radzievskii-Paddack, the names of those who contributed to its discovery.

Chapter 2

General relativistic dynamics

If we wish to further explore the implications of the Poynting-Robertson effect, the obvious case to investigate is how it affects an object caught in a star's gravity well. After all, if the aberration of the radiation field causes every orbiting object to lose energy doesn't that mean that every planet eventually falls into the star?

Describing relativistic effects in a gravitational field requires that we move from the special theory of relativity to the general theory. Though the names are similar, this transition can often be more daunting than the step from non-relativistic to special relativistic physics.

This chapter aims to describe how the kinematic formalism changes from flat to curved space. However, before we can truly treat the physics of curved space we first need the mathematical tools to describe it.

2.1 A little differential topology

To talk about geometry in a general space, we need a rigorous definition of a vector. This is trickier than one might expect if one doesn't have experience with non-euclidean geometry, primarily because the notion of "distance vector" between two points x and y can no longer be given by $x - y$, as one is so used to seeing at the undergraduate level.

The reasoning behind this is that while our coordinate values may live in some region of euclidean $\mathbb{R}^n$ in which addition are allowed, they *map* to different points on a *manifold*. While the points parametrized by the coordinate homotopy $f(s) = xs + (1-s)y$ will follow some line between x and y, there's no guarantee that it will be straight. For example, consider flat polar coordinates: The line drawn along $(r_0 s, 0)$ is a straight radial line, but the polar curve along (r_0, s) is not.

The tangent bundle

Instead, if we want to use vectors, we need to enter the *tangent bundle*. This construct assigns a vector space to each point, allowing us to use vector calculus only to relate vectors *at* that point. This may initially sound like abstract nonsense to a young physics student - vectors *at* a point? But then one realizes that most familiar vectors other than the distance vector - be they magnetic

fields, momentum or spin - are of this type. They have no *end point*, they're merely visualized that way on diagrams at an arbitrary scale. In reality, they are abstract functions associate to a point, and they "live" in its *tangent space*.

There are two common ways to interpret the elements of a tangent space at point labeled by coordinate $\mathbf{x}$.

Germs are equivalence classes of parametrized curves $f(s)$ to the manifold under the equivalence relation $[f] \sim [g] \Leftrightarrow f(0) = g(0), f'(0) = g'(0)$, understood as functions from $\mathbb{R} \mapsto \mathbb{R}^n$, the latter representing the coordinates near $\mathbf{x}$. These tangent vectors are readily understood as four-velocities $\dot{\mathbf{x}}$ along some curve.

Derivations are generated by the linear maps that send scalar functions on the manifold to $\mathbb{R}$ while satisfying Leibniz' product rule. These can be thought of as directional derivatives of the form $v^\mu \frac{d}{dx^\mu}$.

Differential topology is sometimes cited as being the study of things that are invariant under change of notation, and this is a prime example - the two definitions are equivalent. Showing this rigorously takes a few pages[1] of checking well-definedness and other things important to a mathematician, but a physicist should be satisfied noting that in both representations,

$$[f]'(\mathbf{x}) = (x'(0), y'(0), z'(0)) \qquad D_{\mathbf{x}} = (x', y', z') \cdot \nabla \tag{2.1}$$

have the same number of independent parameters.

We can thus use both interpretations at our leisure, allowing us to intuit that one can envision a set of coordinate vectors $(dx_i)^\mu$ defined in the tangent spaces along the trajectory $\dot{x}^\mu$, where they're given by derivations along the coordinates observed in the inertial frame as "directions" rather than realized trajectories.

This means that as soon as we know how to identify an inertial frame in curved space, we can connect our understanding of special relativistic dynamics with the formalism of general spaces.

Covectors and differential n-forms

Before we treat inertial frames, it's worth mentioning one thing mathematicians love above all else: duality. Over the past century, even physicists have begun to develop duality theories, and it's proven a useful tool.

In short, a *dual vector*, sometimes called *covector* or *1-form*, is a linear functional of vectors. By Riesz' representation theorem, the covector space is isomorphic to the vector space, but introducing notation helps reduce the number of mistakes made. In quantum physics, for example, if the *ket*-vector is the vector, then the *bra*-vector is the covector, and together they produce either a scalar or a matrix, much like the index notation does in relativity. In fact, this is precisely where covectors enter our formalism - the *vectors* we know as *contravariant* vectors, while their duals are *covariant* ones. The duality transformation is simply multiplication by the metric.[2]

[1] See, for example, chapter 4 of B. Dundas' *Differential Topology*.

[2] In fact, from a mathematical point of view most of the metrics of physics arise precisely from an inner product structure on the tangent bundle of a finite-dimensional manifold. This explains why we visualize them as coordinate-dependent matrices when a general mathematical metric doesn't have to be.

From the mathematical toolbox of covectors, we attain the concept of *dual coordinate basis*, denoted $(dx_i)_\mu$, which span the cotangent space the same way the coordinate derivatives span the tangent space. From this dual basis we can construct higher n-forms, or completely antisymmetric tensors, by using the *wedge product*:

$$(\omega \wedge \sigma)_{\mu\nu} = \omega_\mu \sigma_\nu - \omega_\nu \sigma_\mu \qquad \textbf{(1-form)} \wedge \textbf{(1-form)} = \textbf{(2-form)} \tag{2.2}$$

$$(\wedge_i^n \omega_{\mu_\mathbf{i}})_{\mu_1,\mu_2,..} = \det(\omega_{\mu_\mathbf{i}}) \qquad \textbf{(Wedge of } \boldsymbol{n} \textbf{ 1-forms)} = \textbf{(}\boldsymbol{n}\textbf{-form)} \tag{2.3}$$

The wedge is a natural generalization of the cross product we know from three dimensions. Through it we can find rigorous notions of *normal vectors* and *volume forms*, the correct quantities to use when evaluating integrals.[3] For instance, in Minkowski space the spatial 3-volume $dV^\mu = \epsilon^{\mu abc} dx_a dy_b dz_c$ represents the normal vector of a three-dimensional surface embedded in four dimensions, which is orthogonal to dx, dy and dz.

Speaking of integrals, the most powerful tool acquired from the mathematics of covectors is the *generalized Stokes theorem*. The theorem relates integral values on a manifold M to integral values on its boundary ∂M, stating that for an $(n-1)$-form ω we have

$$\int_M d\omega = \int_{\partial M} \omega \tag{2.4}$$

Though the d represents a general exterior derivative, for the purposes of any calculations done in this document the theorem can be thought of as the natural extension of the divergence theorem to four dimensions, where it supports our conservation laws. Other special cases include the usual Stokes' theorem for a circle in three dimensions, Green's theorem in two dimensions, and the fundamental theorem of analysis in one dimension.

2.2 The variational principle

One way of defining a straight line between two points is as a trajectory that extremizes the proper distance between them. Given a parametrized line $x(\tau)$ we can integrate a scalar along its trajectory, which in this case is

$$\delta S = \delta \int_{x(\tau)} dS = \delta \int_{x(\tau)} \sqrt{g^{\mu\nu} dx_\mu(\dot{x}) dx_\nu(\dot{x})} = \delta \int_{t_0}^{t_1} \sqrt{g_{\mu\nu} \frac{dx^\mu}{d\tau} \frac{dx^\nu}{d\tau}} d\tau = 0 \tag{2.5}$$

This is analogous to how physically realized trajectories extremize the action in Lagrangian mechanics. The Euler-Lagrange equations that follow from choosing $\frac{dS}{d\tau}$ as a Lagrangian are called the *Geodesic equations*, and assuming the metric to only be coordinate-dependent, they take the form

$$\frac{\partial}{\partial x^\alpha} L = \frac{1}{2L} \left(\frac{\partial}{\partial x^\alpha} g_{\mu\nu} \right) \dot{x}^\mu \dot{x}^\nu \tag{2.6}$$

$$\frac{d}{d\tau} \frac{\partial}{\partial \dot{x}^\alpha} L = \frac{d}{d\tau} \frac{1}{2L} g_{\mu\nu} (\delta^\mu_\alpha \dot{x}^\nu + \dot{x}^\mu \delta^\nu_\alpha) = \frac{d}{d\tau} \frac{1}{2L} \left(g_{\alpha\mu} \dot{x}^\mu + g_{\nu\alpha} \dot{x}^\nu \right) \tag{2.7}$$

[3] Nevertheless, we will keep suppressing the notation if treating it would be a diversion.

By choosing the eigentime parameter τ such that $\frac{dS}{d\tau} = L = 1$ and using the product and chain rules for $\frac{d}{d\tau} g_{\alpha\mu}\dot{x}^\mu = g_{\alpha\mu}\ddot{x}^\mu + \left(\dot{x}^\nu \frac{\partial}{\partial x^\nu} g_{\alpha\mu}\right)\dot{x}^\mu$, we can isolate $\ddot{x}_\alpha$

$$g_{\alpha\mu}\ddot{x}^\mu = \frac{1}{2}\frac{\partial g_{\mu\nu}}{\partial x^\alpha}\dot{x}^\mu\dot{x}^\nu - \frac{1}{2}\dot{x}^\nu\frac{dg_{\alpha\mu}}{dx^\nu}\dot{x}^\mu - \frac{1}{2}\dot{x}^\mu\frac{dg_{\nu\alpha}}{dx^\mu}\dot{x}^\nu \tag{2.8}$$

This is commonly written in terms of the *Christoffel symbols*, denoted $\Gamma^\alpha_{\mu\nu}$

$$\Gamma^\alpha_{\mu\nu} \equiv \frac{1}{2} g^{\alpha\lambda}\left(\partial_\mu g_{\lambda\nu} + \partial_\nu g_{\mu\lambda} - \partial_\lambda g_{\mu\nu}\right) \tag{2.9}$$

$$\Rightarrow \frac{d\dot{x}^\alpha}{d\tau} = -\Gamma^\alpha_{\mu\nu}\dot{x}^\mu\dot{x}^\nu \tag{2.10}$$

Trajectories $x^\mu(\tau)$ that satisfy the geodesic equation are called *geodesics*, and serve as our definition for straight lines. In a space curved by gravity, these are the physically realized trajectories. Gravity is no longer a force, but rather a re-definition of straightness. The non-Euclidean nature is revealed by realizing that straight lines can now intersect at more than one point. For instance, polar and azimuthal orbits around the Earth intersect twice, which violates the parallel postulate of Euclidean geometry.

Since the equivalence principle equates observed acceleration with gravity, a freely falling observer would need to observe vanishing Christoffel symbols in their locally Cartesian reference frame. Thus, this re-definition is sometimes counter-intuitive: It implies that someone jumping in a parabola is following a straight line, while someone standing still or walking on the ground is not.

2.3 Curved lines in curved space

Of course, not all lines are straight. Systems that experience non-gravitational forces are accelerated due to other effects than the curvature of space, and we need a formalism that handles both straight and curved lines, like we're used to from flat space.

The covariant derivative

Partial derivatives, as we're used to seeing them, are usually thought of as "rate of change along the coordinate axis". However, there's no guarantee that the coordinate axis will be a straight line. In 2D flat space given by polar coordinates, for instance, the trajectory $(r, \theta) = (r_0, \omega\tau)$ following the polar angle is not straight. That trajectory follows $\ddot{x} = 0$, and so requires something which compensates for the Christoffel symbols in eq. (2.10).

In order to compute "straight" differentials independent of coordinate systems, we introduce the *covariant derivative*, denoted D_μ. It corresponds to the usual coordinate gradient for scalars, but is defined on tensorial quantities in terms of the coordinate derivatives *and* Christoffel symbols:

$$D_\mu v^\alpha = \partial_\mu v^\alpha + \Gamma^\alpha_{\mu\nu} v^\nu \tag{2.11}$$

$$D_\mu v_\nu = \partial_\mu v_\alpha - \Gamma^\alpha_{\mu\nu} v_\alpha \tag{2.12}$$

$$D_\mu v^{\alpha\beta..}_{\sigma\lambda..} = \partial_\mu v^{\alpha\beta..}_{\sigma\lambda..} + \left(\Gamma^\alpha_{\mu\nu} v^{\nu\beta..}_{\sigma\lambda..} + \Gamma^\beta_{\mu\nu} v^{\alpha\nu..}_{\sigma\lambda..} + ..\right) - \left(\Gamma^\nu_{\mu\sigma} v^{\alpha\beta..}_{\nu\lambda..} + \Gamma^\nu_{\mu\lambda} v^{\alpha\beta..}_{\sigma\nu..} + ..\right) \tag{2.13}$$

summed over contravariant indices and subtracted over covariant indices, which corresponds to whether one would use a coordinate transform or its inverse to generalize its rest-frame quantity.

For a 1-vector, this looks somewhat familiar. Indeed, using D_μ and the chain rule for $\frac{d}{d\tau} = \dot{x}^\mu \frac{\partial}{\partial x^\mu}$, the geodesic equation is simplified to

$$D_\tau \dot{x}^\alpha = \dot{x}^\mu D_\mu \dot{x}^\alpha = 0 \tag{2.14}$$

which looks oddly like Newton's first law: an object experiencing no covariant acceleration moves in a straight line.

On an intuitive level, replacing d_τ with D_τ respects a tensor's status as a local quantity by generating translations in some direction $\dot{x}$. A vector is moved to another tangent space by managing the effects of curvature and choice of coordinate system - things that are more mathematical artifacts than physically measurable quantities.

Newton's laws

If there *is* a physical acceleration occurring from some source other than gravitation, the geodesic equation $D_\tau \dot{x}^\mu = 0$ no longer holds, and the lines are no longer straight. Fortunately, the covariant derivative allows for a covariant formulation of Newton's laws, which is satisfyingly similar to what we're used to.

1. In the absence of forces, $D_\tau p^\mu = 0$.
2. Force is mass[4] times acceleration, $F^\mu = mA^\mu = mD_\tau \dot{x}^\mu$.
3. Total four-momentum is conserved, $D_\tau p^\mu_{\text{tot}} = 0$.

It's worth remembering that vectorial quantities like the four-momentum mathematically live in the tangent spaces of each point, and so their conservation law is intrinsically local. Two trajectories - for instance, a circular orbit and an elliptic one - may intersect at two different points and observe a change in the other's relative momentum even though neither experienced any force.

In chapter 3 we'll see how to define the momentum flow in terms of the *energy-stress tensor* $T^{\mu\nu}$, for which Newton's third law becomes a divergence relation of the form $D_\nu T^{\mu\nu} = 0$.

Example: Forces in a co-rotating frame

One benefit of the covariant formalism is that the four-force always transforms as a vector under coordinate transforms; any special treatment warranted by choosing non-inertial coordinates is tucked into the Christoffel symbols. To exemplify this, we will transform a force vector from a co-rotating Cartesian frame to polar coordinates in flat space.

What this means is that around any given point (r_0, θ_0) we define a locally Cartesian coordinate system (x, y) aligned along the $\partial\hat{r}$ and $r_0\partial\hat{\theta}$ direction, i.e. $(x, y) = (r_0 + a\partial\hat{r}, r_0\theta_0 + br_0\partial\hat{\theta})$.

[4] Assuming constant rest energy, no thermal fluctuations.

Now, assuming we have a force vector (F^x, F^y) in a frame at (r, θ), one might think of the calculation

$$\dot{y} = r\dot{\theta} + \dot{r}\theta \qquad\qquad \ddot{y} = r\ddot{\theta} + 2\dot{\theta}\dot{r} + \ddot{r}\theta \tag{2.15}$$

and conclude that solving this equation for $\ddot{\theta}$ and inserting $\ddot{y} = F^y/m$ gives you the expression for F^θ/m. This is what one would do in non-relativistic mechanics, giving rise to concepts like the Coriolis effect and Centrifugal forces.

Were we to insert this solution as a force in the covariant version of Newton's second law, however, we would run into issues, because the extra terms are already taken care of by the Christoffel symbols in the covariant derivative. Including them on both sides of the equality sign would double their contribution!

In this age of computer-aided Christoffel symbol handling, the lesson to be learned is that one shouldn't over-think things and simply use the general transformation rule for vectors:

$$F^r = \frac{\partial r}{\partial x^\mu} F^\mu = F^x \qquad\qquad F^\theta = \frac{\partial \theta}{\partial x^\mu} F^\mu = \frac{1}{r} F^y \tag{2.16}$$

2.4 Rotation and torques

If our goal was to treat the many kinds of rotation from section 1.3, we would need a framework to treat angular momentum. Classically, this is given by

$$\vec{J} = \vec{r} \times \vec{p} \tag{2.17}$$

As mentioned at the start of this chapter, the cross product on a three-dimensional manifold is a wedge product of 1-forms into a 2-form, but by Hodge $\star$-duality[5] it's still representable as a unique vector in 3-space. This is how we often choose to visualize angular momentum in classical mechanics. In four dimensions, however, there is no unique axis orthogonal two the two vectors, and so 2-forms remain 2-forms.

In addition, it is only in a Cartesian inertial frame that we can treat the coordinate separation from the center of mass as a vector Δx^μ, where the angular momentum is defined as the wedge product

$$J^{\mu\nu} = \mathbf{\Delta x} \wedge \mathbf{p} = \Delta x^\mu p^\nu - \Delta x^\nu p^\mu \tag{2.18}$$

Similarly, if we recall the classical expression for torques

$$\vec{M} = \vec{r} \times \vec{F} \tag{2.19}$$

[5]The physicist's way of interpreting Hodge $\star$-duality is to note that an anti-symmetric 3×3 matrix has 3 independent parameters, same as a 3-vector, and one transforms between the two by contracting with the Levi-Cevita tensor when calculating the cross product. For a 4×4 matrix, it's 6, which cannot be listed as a 4-vector. Rigorously, Hodge $\star$-duality is an equivalence between n-forms and $(d-n)$-forms on a d-dimensional smooth manifold such that $\langle a| \wedge \langle \star b| = \langle a|b\rangle \langle d^d V|$. For details consult the problems section of Madsen and Tornehave's book on differential topology, *From Calculus to Cohomology* (1997).

we generalize to

$$M^{\mu\nu} = \Delta x^\mu F^\nu - \Delta x^\nu F^\mu \tag{2.20}$$

It's worth remembering that in general curved space the coordinate list x^μ is not necessarily a vector even though $\dot{x}^\mu$ is, so the above must be derived in a local frame before transforming to the curved-space generalization, and non-local objects are often problematic since any response to a force will propagate through a medium at most the speed of light.

Nevertheless, there can be macroscopic conservation laws that behave like conservation of angular momentum. If a general metric has a symmetry it gives rise to a Killing vector η such that the inner product $\eta_\mu \dot{x}^\mu$ along any geodesic $\dot{x}^\mu$ is conserved.

Thus, in axisymmetric geometries there exists a conserved quantity sometimes used to describe the orbital angular momentum of point-particles:

$$l \equiv m\eta_\mu \dot{x}^\mu \tag{2.21}$$

where η is the Killing vector associated to the metric's independence on polar angle. In the Schwarzschild geometry with the usual coordinates the Killing vector of ϕ is $\eta^\mu = (0, 0, 0, 1)$, making the polar angular momentum around the equator be $l = mg_{\phi\phi}\dot{\phi} = mr^2\dot{\phi}$, which agrees with classical results.

Thus, there are methods that work for both rotational and orbital angular momenta, with the caveat that if a body is spinning on the scale where relativistic effects are relevant, most rigid materials will rip themselves asunder. Only massive stars and black holes are able to endure the high stresses that come with relativistic rotation.

Chapter 3

The Stress-Energy Tensor

The elements of the Stress-Energy tensor, which is usually denoted $T^{\mu\nu}$, can be thought of as generalized momentum flux densities, where energy is considered as the time-component of the four-momentum. In Cartesian coordinates it's easily interpreted as

$$T^{\mu\nu} = \frac{dP^\mu}{d^4V}dx^\nu = \left(\begin{array}{c|c} \text{Energy density} & \text{Energy flux} \\ \hline \text{Momentum densities} & \text{Stress tensor} \end{array}\right) \tag{3.1}$$

In natural units, this can be shown to be a symmetric tensor. We note that the time-indexed elements are simply the spatial three-densities of the four-momentum, and the spatially indexed components are force two-densities, i.e. the pressures and stresses we know from the classical theory. These can be recovered by applying the tensor to a normal vector in the relevant direction, so in accordance with the last chapter we have

$$dp^\mu = T^{\mu\nu}u_\nu dV \qquad\qquad dF^i = T^{i\nu}n_\nu dA \tag{3.2}$$

where u_ν refers to the four-velocity of the 3-surface in question, not its content. It's worth noting that the net force acting on the surfaces an enclosed volume requires a compatible orientation of the normal vectors, and any physical test surface aiming to measure the net dynamic force needs to have an infinitesimal thickness dl. Such a test surface experiences

$$F_{\mathbf{Surf}} = \left(T^{i\nu}(x+dl) - T^{i\nu}(x)\right)n_\nu dA \tag{3.3}$$

$$= \left(\frac{dT^{i\nu}}{dx}dl\right)n_\nu dA \tag{3.4}$$

which relates nicely to the language of non-relativistic stress and strain used in fluid mechanics and elastics. In this sense any constant stress-energy tensor is static, and a test surface that doesn't directly interfere by changing the stress-energy tensor by its presence will not be accelerated.

Conservation of energy-momentum

From eq. (3.2) we see that forces and momenta are related through the stress tensor, and we may wonder if we can find a way to interpret the conservation laws for energy-momentum in it. The answer is yes, we can.

Using the interpretations of eq. (3.1), conservation of energy means that the time-derivative of the energy of any given test volume must be balanced by the energy flux out of it, so we immediately find $\partial_\mu T^{\mu 0} = 0$. Similar arguments hold for each component of the four-momentum, so in other words

$$\partial_\mu T^{\mu\nu} = 0 \tag{3.5}$$

We only really know this to be true in inertial frames, in accordance with special relativity. Luckily, we know from chapter 2 how to compute derivatives along a geodesic using the covariant derivative, so this conservation law can be transformed to arbitrary non-inertial coordinates as

$$D_\mu T^{\mu\nu} = D_\nu T^{\mu\nu} = 0 \tag{3.6}$$

which represents the *local* conservation of energy-momentum. This is subtly different from an absolute conservation law, as it allows us to model phenomena such as the expansion of the universe, where observed energy densities may be decreasing in response to the dynamic space-time.

Angular momentum density

Using eq. (3.2), the familiar angular momentum (2.18) and torque (2.20) of an object in its rest frame can be expressed in terms of the stress-energy tensor:

$$\mathcal{J}^{\mu\nu\alpha} \equiv dx^\mu T^{\nu\alpha} - dx^\nu T^{\mu\alpha} \tag{3.7}$$

$$J^{\mu\nu} = \int \mathbf{dx} \wedge \mathbf{dp} = \int \mathcal{J}^{\mu\nu\alpha} u_\alpha d^3V \tag{3.8}$$

$$M^{\mu\nu} = \int \mathbf{dx} \wedge \mathbf{dF} = \int \mathcal{J}^{\mu\nu\alpha} n_\alpha d^2A \tag{3.9}$$

The angular momentum density inherits its conservation law from conservation of the stress-energy tensor:

$$D_\alpha \mathcal{J}^{\mu\nu\alpha} = 0 \tag{3.10}$$

Though we will not be making much use of angular momentum in this document, it's satisfying to know that a formalism for it exists.

3.1 The Poynting-Robertson effect revisited

With the energy-stress tensor and covariant formalism in hand, we can now revisit the example from section 1.1 with a stress tensor of the form $T^{\mu\nu} = W\lambda^\mu\lambda^\nu$, where $\lambda^\mu = (1, 1, 0, 0)$ is a tangent vector for the photons in the stellar frame.

Black body absorption with isotropic emissions

A small black body with high conductivity can to a good approximation be assumed to radiate isotropically. In reality it will never be quite true, of course, but it simplifies the model a fair bit.

In the context of a uniform ensemble of photons, the force elements of the stress-energy tensor can be thought of as a measure of photon momenta crossing a surface in the given direction per unit of time. A black body can be considered to be undergoing inelastic collisions with all these, completely absorbing their 3-momenta. In other words, the force experienced by a black surface element dA with normal n_ν is given as

$$dF^i = T^{i\nu} n_\nu dA \tag{3.11}$$

Assuming isotropic emission from the rest frame during black body radiation, some relativistic beaming may be observed, but this will exert no net 3-force on the remaining mass. Conservation of energy in the rest frame allows us to verify the necessity of an extra term to arrive at a covariant formula,

$$dF^\mu = (g^\mu_\lambda - u^\mu u_\lambda) T^{\lambda\nu} n_\nu dA \tag{3.12}$$

which in the rest frame equates to projecting onto the spatial parts. If $T^{\mu\nu} = W\lambda^\mu\lambda^\nu$ as in chapter 1.2, this formula immediately produces the expected results - with the benefit of being usable in any geometry and for any shape!

Perfect reflection

Until now we've only treated the movement of black bodies, but those are not our only options! A real object will experience partial absorption and partial reflection, so we need to investigate how reflection works.

We know the photon flux density from $T^{\mu\nu}$, so we'll first investigate how a single photon Compton scatters off a massive particle.

Denote the pre-collision variables by greek letters and the post-collision ones by latin, with the exception of m, μ, θ and ϕ, which are the invariant mass, index, and angles.

Conservation of four-momentum reads

$$\pi^\mu + \omega^\mu = (\epsilon + \omega, \vec{\pi} + \vec{\omega}) = (E + f, \vec{p} + \vec{f}) = p^\mu + f^\mu \tag{3.13}$$

from which we derive

$$\Delta P^\mu \equiv p^\mu - \pi^\mu = \omega^\mu - f^\mu \tag{3.14}$$

$$\begin{aligned} \Delta P_\mu \Delta P^\mu = m^2 - 2\pi_\mu p^\mu + m^2 &= 0 - 2\omega_\mu f^\mu + 0 \\ &= 2m^2 - 2E\epsilon + 2p\pi\cos\phi \\ &= -2f\omega + 2f\omega\cos\theta \end{aligned} \tag{3.15}$$

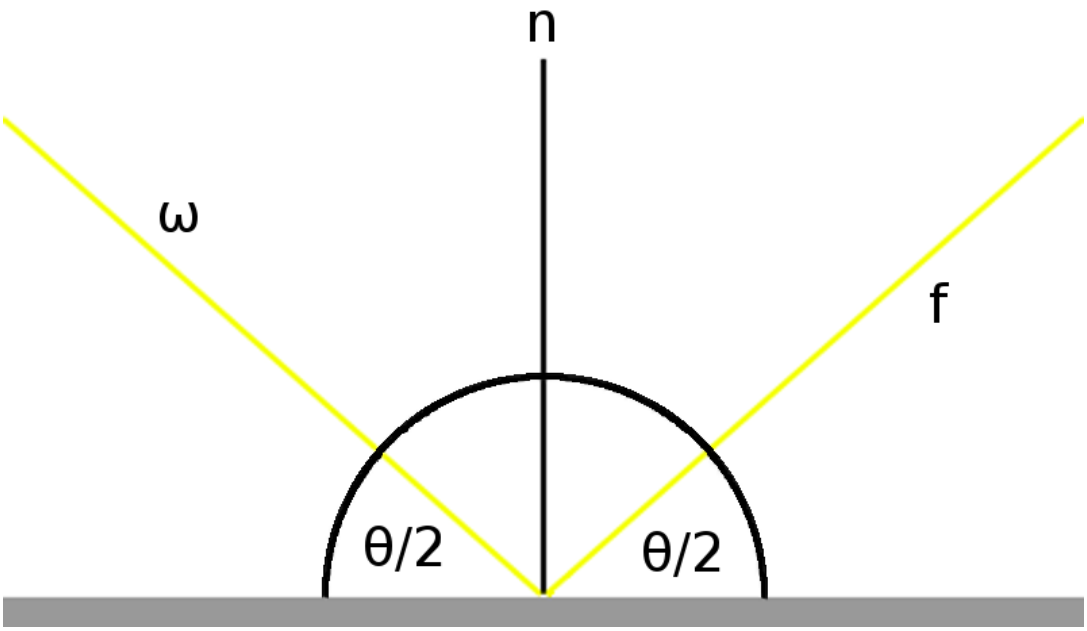

Figure 3.1: Compton scattering off a heavy reflective surface.

Next, consider the massive particle's rest frame system, where $\vec{\pi} = \vec{0}, \epsilon = m$

$$m^2 - Em = -m\Delta P^0 = m(f - \omega) = -f\omega(1 - \cos\theta) \tag{3.16}$$

$$\Rightarrow f = \left(\frac{1}{\omega} + \frac{1}{m}(1 - \cos\theta)\right)^{-1} = \frac{\omega}{1 + \frac{\omega}{m}(1 - \cos\theta)} \tag{3.17}$$

In order to use this to calculate the momentum transfer per photon, we define $c = (1 - \cos\theta)/m$ to compactify our notation.

$$\omega - f = E - m = \sqrt{p^2 + m^2} - m \tag{3.18}$$

$$\begin{aligned} p^2 &= (\omega - \frac{\omega}{1 + \omega c} + m)^2 - m^2 \\ &= \left(\left(\frac{\omega^2 c}{1 + \omega c} + m\right)^2 - m^2\right) \\ &= \frac{\omega^4 c^2 + 2\omega^2 mc(1 + \omega c)}{(1 + \omega c)^2} \end{aligned} \tag{3.19}$$

which, in the limit where $m \gg \omega$, is to a good approximation

$$\approx 2\omega^2(1 - \cos\theta) \Rightarrow |p| = 2\omega \sin\left(\frac{\theta}{2}\right) = 2\vec{\omega} \cdot \hat{n} \tag{3.20}$$

where $\hat{n}$ is the normal of the reflective surface, along which the momentum is transferred. Note that this means a simple inclined plane can provide thrust sideways, like a sail. In terms of the stress-energy tensor the total momentum flux on a surface element is then given

$$dF^\lambda = 2n^\lambda n_\mu T^{\mu\nu} n_\nu dA \tag{3.21}$$

These are the primary models we will treat in chapter 4 and 5.

3.2 The Einstein field equations

Lastly, the Einstein field equations, or EFE for short, describe how the stress-energy-tensor gives rise to the curvature of space. While its derivation can take an entire book, it's commonly formulated in natural units where Newton's gravitational constant $G_N = 1$ and the speed of light $c = 1$ as

$$G_{\mu\nu} = 8\pi T_{\mu\nu} \tag{3.22}$$

where $G_{\mu\nu}$ is a complicated measure of curvature derived from the metric through the covariant derivative. Solving the EFE exactly is a rare occurrence, and for the purposes of this document it will suffice to consider the *linearized* field equations, where the stress-energy is related to the metric perturbation $h_{\mu\nu}$ such that $g_{\mu\nu} = \eta_{\mu\nu} + h_{\mu\nu}$ by either of

$$\Box \left(h_{\mu\nu} - \frac{h^\alpha_\alpha}{2}\eta_{\mu\nu} \right) = 8\pi T_{\mu\nu}. \tag{3.23a}$$

$$\Box h_{\mu\nu} = 8\pi T_{\mu\nu} - 4\pi T^\alpha_\alpha \eta_{\mu\nu} \tag{3.23b}$$

The common notation defines the trace-reversed version of either side by $\bar{h}_{\mu\nu} = h_{\mu\nu} - \frac{1}{2}h^\alpha_\alpha \eta_{\mu\nu}$ and $\bar{T}_{\mu\nu} = T_{\mu\nu} - \frac{1}{2}T^\alpha_\alpha \eta_{\mu\nu}$.

The linearized equations are a fair approximation as long as $h_{\mu\nu} \ll \eta_{\mu\nu}$. Furthermore, it is often analytically solvable, with the general solution provided in section 23.3 of Hartle[1] as

$$\bar{h}^{\mu\nu}(t, x) = 4 \int d^3x' \frac{T^{\mu\nu}(t - |x - x'|, x')}{|x - x'|} \tag{3.24}$$

as a perturbation to Cartesian flat space.

For either set of equations, one thing is clear: Curvature can arise as a consequence of velocity through the momentum densities. A rotating star, for instance, doesn't curve space-time only through the gravitational potential of its mass-energy, but also the momentum of its rotation. This result is what turns the Schwarzschild metric into the Kerr metric, where a gravitomagnetic drag arises due to the star's angular momentum.

The way a Lorentz boost affects a diagonal stress-energy by generating off-diagonal terms. We therefore expect any velocity-dependent metrization of the stress to appear as the g_{0i}-terms that mix time and space, which seems intuitive. With that in mind, it appears plausible that we can emulate viscosity through the metric, though the exact form requires a little more calculation.

Still, for matter moving at speeds low compared to the speed of light the spatial momentum is small compared to the mass, which supports the model of matter-dominated stress-energy as approximately $\mathrm{diag}(\rho, 0, 0, 0)$ for the purposes of generating curvature. On the other hand, a radiation fluid behaves precisely opposite - the stress-energy is the same in every direction, supporting the pattern $\mathrm{diag}(\rho, \frac{\rho}{3}, \frac{\rho}{3}, \frac{\rho}{3})$.

We thus see that the two models generate curvature in different ways. Dust generates equal contributions to space and time through the non-zero trace, while radiation is traceless and contributes three times more to the time-component of the metric than the spatial components.

Chapter 4

Near a Schwarzschild star

In the last chapter we learned how to compute the interaction of the stress-energy tensor of a uniform radiation field with black and reflective surfaces in locally flat space. However, the true test of the accrued formalism comes in curved space, and the natural geometry to investigate is the geometry near a point-mass, represented by the Schwarzschild metric

$$g_{\mu\nu}dx^\mu dx^\nu = \left(1 - \frac{2M}{r}\right) dt^2 - \left(1 - \frac{2M}{r}\right)^{-1} dr^2 - r^2\left(d\phi^2 + \sin^2\phi d\theta^2\right) \quad (4.1)$$

Since this geometry is spherically symmetric and we don't expect any azimuthal forces to appear, we can restrict our computation to the equatorial $(2+1)$-dimensional slice of space-time (t, r, θ) for which the metric is simply

$$g_{\mu\nu} = \text{diag}\left(\left(1 - \frac{2M}{r}\right), -\left(1 - \frac{2M}{r}\right)^{-1}, -r^2\right) \quad (4.2)$$

In order to relate the rest-frame force vector to Schwarzschild coordinates, we can further introduce co-rotating locally Minkowski frames where $(dt, dx, dy) = (dt, dr, rd\theta)$ near each point as described in section 2.3, thereby maintaining the simple representation of $T^{\mu\nu}$ for a radial photon flow and allowing us to compute Lorentz transforms in these frames using $(\dot{t}, \dot{x}, \dot{y}) = (\dot{t}, \dot{r}, r\dot{\theta})$ such that $\dot{y}$ corresponds to an orbital velocity. This is useful when it comes to transforming the normal vectors on the surface of the object to their moving frames, which is needed to compute the inner product terms of chapter 3.

Using index-less simplified notation eq. (3.12) and eq. (3.21), describing the forces experienced by black and reflective surface elements in the co-rotating stellar frame, can be written

$$dF_{\mathbf{B}} = (1 - uu^\dagger)T(\Lambda\hat{n})dA \quad (4.3)$$

$$dF_{\mathbf{R}} = \Lambda^{-1}\hat{n}\left((\Lambda\hat{n})^\dagger T(\Lambda\hat{n})\right)dA = \Lambda^{-1}\hat{n}(\hat{n}(\Lambda T\Lambda)\hat{n})dA \quad (4.4)$$

where Λ refers to the Lorentz transformation from the stellar frame to the object's frame, T is the stress-energy tensor, u is the four-velocity and $\hat{n}$ is the normal vector of the sunward-pointing surface to integrate over. The resulting vector is the total force experienced due to radiation in the co-rotated frame at

rest with respect to the stellar frame. If further transformed back to spherical coordinates, the geodesic equation is modified to

$$\ddot{x}^\alpha = -\Gamma^\alpha_{\mu\nu}\dot{x}^\mu\dot{x}^\nu + F^\alpha \tag{4.5}$$

where we learned how to calculate $\Gamma^\alpha_{\mu\nu}$ from the metric in chapter 2.

$$\Gamma_{0\mu\nu} = \begin{pmatrix} 0 & \frac{M}{r^2} & 0 \\ \frac{M}{r^2} & 0 & 0 \\ 0 & 0 & 0 \end{pmatrix}, \quad \Gamma_{1\mu\nu} = \begin{pmatrix} \frac{-M}{r^2} & 0 & 0 \\ 0 & \frac{M}{(r-2M)^2} & 0 \\ 0 & 0 & r \end{pmatrix}, \quad \Gamma_{2\mu\nu} = \begin{pmatrix} 0 & 0 & 0 \\ 0 & 0 & -r \\ 0 & -r & 0 \end{pmatrix} \tag{4.6}$$

For complicated shapes, the surface integrals for the radiation force can be somewhat computationally heavy. The simplest shapes, which will be modelled in this chapter, are a sphere and a co-rotating, approximately cubical object with surface normals aligned in the $\hat{r}$ and $\hat{\theta}$ directions.

To verify that we achieve the special case of the Poynting-Robertson effect as predicted in section 1.2, we let Maple calculate the force for cubes and a sphere in the co-rotating frame, then simplifying the equation by setting $\dot{r} = 0$.

$$F^\mu_{\mathbf{S}} = \frac{WA}{r^2}\begin{pmatrix} -\gamma\dot{y}^2 \\ \gamma \\ -\gamma^2\dot{y} \end{pmatrix} \qquad \textbf{(Black sphere)} \tag{4.7}$$

$$F^\mu_{\mathbf{R}} = \frac{WA}{r^2}\begin{pmatrix} -2\dot{y}^3 \\ 2 \\ -2\gamma\dot{y}^2 \end{pmatrix} \qquad \textbf{(Reflective cube)} \tag{4.8}$$

$$F^\mu_{\mathbf{B}} = \frac{WA}{r^2}\begin{pmatrix} -\dot{y}^3 - \dot{y}^2 \\ \dot{y} + 1 \\ -\gamma\left(\dot{y}^2 + \dot{y}\right) \end{pmatrix} \qquad \textbf{(Black cube)} \tag{4.9}$$

Were it not for the linear term, the forces experienced by the cubes would be proportional, as they are for the black cube and sphere.

$$F^\mu_{\mathbf{B}} = \frac{1+\dot{y}}{\gamma}F^\mu_{\mathbf{S}} = \frac{1}{2}F^\mu_{\mathbf{R}} + \frac{WA}{r^2}\begin{pmatrix} -\dot{y}^2 \\ \dot{y} \\ -\gamma\dot{y} \end{pmatrix} \tag{4.10}$$

Similarly, to verify that we achieve the Doppler effect we set $\dot{\theta} = 0$.

$$F_{\mathbf{S}} = F_{\mathbf{B}} = \frac{1}{2}F_{\mathbf{R}} = \begin{pmatrix} -\dot{x}(\gamma - \dot{x})^2 \\ \gamma(\gamma - \dot{x})^2 \\ 0 \end{pmatrix}\frac{WA}{r^2} \tag{4.11}$$

This looks reasonable - the frequency of each photon is shifted by as much as the frequency of photon encounters. Following the calculations of section 1.2 the observed 3-acceleration simply becomes $a_\parallel = (1-v)^2$, for which the corrective term is of lowest-order $-2v$, making the trajectory more resistant to radial perturbations than orbital.

These expressions can easily be included in the geodesic equations as a four-force by applying the coordinate transformation back to spherical coordinates. However, which parameters are appropriate to choose?

4.1 Effective cross-sections

The importance of the Poynting-Robertson effect can depend on several circumstantial parameters, but the most intuitive one is the ratio of radial radiation force to Newtonian gravitational force $\alpha = \frac{F_{\mathbf{rad}}}{F_{\mathbf{grav}}} \approx \frac{WA}{GMm}$, which in natural units of solar masses simplifies to the $\frac{WA}{m}$ that appears in eq. (1.9). Along with the velocity-dependent ratio of radial to orbital cross-section for a given type of object this is sufficient to describe all the radiation-dependent forces.

However, the effective radial cross-section has consequences not only for the Poynting-Robertson effect, but also for stable orbits. If the radial pressure is strong enough, α will compensate sufficiently for gravity that an otherwise circular orbit will exceed the escape velocity of the reduced effective potential.

To see when this happens, we can compare the Newtonian orbital and escape velocities with or without radiation:

$$v_{\mathbf{orbit}} = \sqrt{\frac{GM}{r}} \mapsto \sqrt{\frac{GM(1-\alpha)}{r}} \tag{4.12}$$

$$v_{\mathbf{escape}} = \sqrt{\frac{2GM}{r}} \mapsto \sqrt{\frac{2GM(1-\alpha)}{r}} \tag{4.13}$$

In general, we can use the Kepler formalism for an elliptic orbit of eccentricity e starting at its perihelion to calculate the reach of a vessel with cross-section α leaving a circularly orbiting planet.

$$v_{\mathbf{per}} = \sqrt{\frac{GM}{r}} \equiv \sqrt{\frac{(1+e)(1-\alpha)GM}{r_{\mathbf{per}}}} \Rightarrow 1 + e = \frac{1}{1-\alpha} \tag{4.14}$$

$$\Rightarrow r_{\mathbf{api}} = r_{\mathbf{per}} \frac{1+e}{1-e} = r_{\mathbf{per}} \frac{\frac{1}{1-\alpha}}{2 - \frac{1}{1-\alpha}} = \frac{r_{\mathbf{per}}}{1-2\alpha} \tag{4.15}$$

So to leading order, the normal orbital velocity overtakes the effective escape velocity when $\alpha = 0.5$, which we will call the *critical cross-section*. This is what a radiation-powered craft leaving a normal orbit would need to escape the gravity well. If $\alpha = 1$, we call it *supercritical*. This is when the net radial force reverses, the sun becomes repulsive, and there are no possible stable orbits. Since both the classical gravitational pull and the radiation pressure decay as $1/r^2$, this observation is approximately radius-independent.[1]

Relative cross-sections

Having established this range of interesting parameters for radial pressure, we can now further investigate how the Poynting-Robertson effect relates to it. Since our test surfaces are symmetrically aligned, we have relatively simple velocity-dependent expressions for the ratio of orbital to radial force:

$$\beta = \frac{F^y}{F^x} = \begin{cases} -\gamma^2 v = & -v + \mathcal{O}(v^3) & \textbf{(Black sphere)} \\ -\gamma^3 v^2 = & -v^2 + \mathcal{O}(v^4) & \textbf{(Reflective cube)} \\ -\gamma^2 v = & -v + \mathcal{O}(v^3) & \textbf{(Black cube)} \end{cases} \tag{4.16}$$

[1] As long as $r \gg M$ at least.

Thus, to leading order in v, the orbital force in a circular orbit adjusted for radial pressure depends on α and the radius as

$$F^y = \beta\alpha\frac{Mm}{r^2} \propto \begin{cases} \frac{v\alpha}{r^2} \propto \frac{\alpha\sqrt{1-\alpha}}{r^{2.5}} & \textbf{(Black)} \\ \frac{v^2\alpha}{r^2} \propto \frac{\alpha-\alpha^2}{r^3} & \textbf{(Reflective)} \end{cases} \tag{4.17}$$

with cross-sectional maxima at $\alpha = \frac{2}{3}$ and $\alpha = 0.5$, respectively. The radius-dependence makes it clear that these would only be comparable close to the Schwarzschild radius. Nevertheless, the radius deficit Δr per orbit increases since the effective Newtonian energy is $\frac{(\alpha-1)M}{2r}$, meaning

$$\Delta E \approx F^y \cdot 2\pi r \approx \frac{(1-\alpha)Mm}{2r^2}\Delta r = \frac{1-\alpha}{2}\frac{F^x}{\alpha}\Delta r \tag{4.18}$$

$$\Rightarrow \frac{\Delta r}{r} = 4\pi\frac{\beta\alpha}{1-\alpha} \propto \begin{cases} \frac{\alpha}{\sqrt{r-\alpha r}} & \textbf{(Black)} \\ \frac{\alpha}{r} & \textbf{(Reflective)} \end{cases} \tag{4.19}$$

For elliptic orbits one can go through similar calculations, but the interesting observations can be made entirely qualitatively. Since the radius-dependence of the orbital force is of a higher negative order than gravity, the energy loss near the perihelion, where the orbital velocity exceeds circular parameters, is greater than that near the apihelion, where the situation is reversed. This reduces the eccentricity of the orbit with every pass.

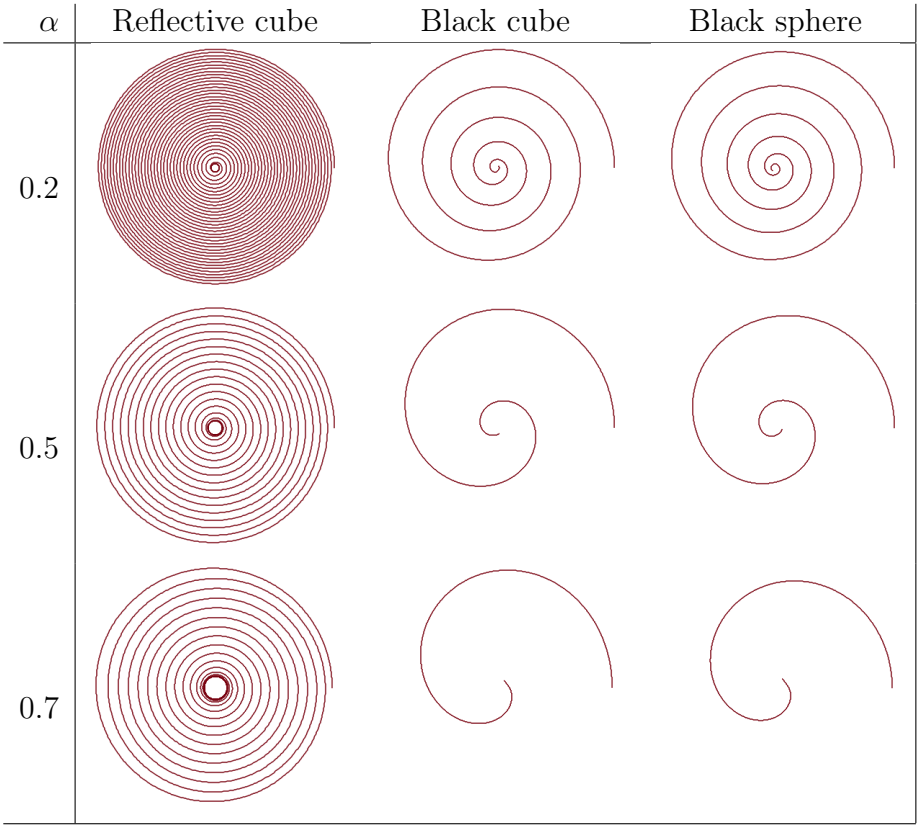

Figure 4.1: Decaying Poynting-Robertson trajectories starting at $100M$ distance with an adjusted initial orbital velocity $v_0 = 0.1\sqrt{1-\alpha}$, which would be appropriate for a Newtonian circular orbit in the absence of relativistic corrections.

In fig. 4.1 we see the Poynting-Robertson effect in practice for a Schwarzschild geometry and symmetrically shaped objects. Even for objects with critical radial cross-sections slow orbits do exist, but due to the shapes these are eventually caught by the orbital friction.

It's worth noting that a reflective surface, which experiences twice the radial pressure and only higher-order orbital decay, reaches critical cross-sections much easier. As briefly mentioned in section 3.1, inclined reflective sails are even capable of providing orbital thrust depending on their alignment, easily overcoming the Poynting-Robertson effect.

Scale bias of radiation pressure

Generally, naturally occurring objects in space tend to be symmetric enough to approximate the volume as $\propto r^3$ and cross-section as $\propto r^2$. This implies that

$$\alpha \propto \frac{A}{m} \propto \frac{r^2}{\rho r^3} = \frac{1}{\rho r} \tag{4.20}$$

meaning large symmetric objects such as planets are mostly unaffected by radiation pressure. On the other hand, small objects such as motes of dust or ice falling off comets are more easily affected. Depending on their initial velocity and cross-section, these either get launched out of the solar system on a hyperbolic orbit or eaten by the Poynting-Robertson effect, effectively cleaning the dust from stable, circular orbits and leaving mostly solid macroscopic objects.

Planet	α	Body	α
Mercury	$4.8{\cdot}10^{-14}$	Pluto	$3.3\cdot10^{-13}$
Venus	$3{\cdot}10^{-14}$	Ceres	$6.3\cdot10^{-13}$
Earth	$2.23{\cdot}10^{-14}$	2 Pallas	$9.2\cdot10^{-13}$
Mars	$4.99\cdot10^{-14}$	4 Vesta	$9\cdot10^{-13}$
Jupiter	$9.2\cdot10^{-15}$	10 Hygiea	$1\cdot10^{-12}$
Saturn	$2\cdot10^{-14}$	624 Hektor	$3.1\cdot10^{-12}$
Uranus	$2.7\cdot10^{-14}$	951 Gaspra	$4.3\cdot10^{-12}$
Neptune	$2\cdot10^{-14}$	25143 Itokawa	$1.2\cdot10^{-8}$

Data source: WolframAlpha Knowledgebase, 2015

Table 4.1: First-order force ratio estimates assuming a sphere model with $\alpha = (1+a)\frac{L_\odot r_\oplus^2}{4GM_\odot m_\oplus c}$ where a is the albedo. As expected, smaller objects are more affected, but none approach critical values.

This also means only certain kinds of interstellar dust that enter the solar system are likely to remain. Too small, and the sun becomes repulsive. Too large, and an initially positive-energy hyperbolic trajectory is unlikely to lose sufficient energy in one pass to cross the energy threshold and be caught.

From the analysis of elliptic orbits losing eccentricity, it seems intuitive that the kind of dust most likely to be caught should have a near-critical cross-section and be on an initially slow hyperbolic trajectory which takes it close to the sun.

4.2 Radiation pressure in the Solar system

We may be curious to what degree radiation pressure affects us and the future of our space exploration. If we stop using natural units and insert table values, the critical mass area density for a reflective surface is $\frac{m}{A} = \frac{2L_\odot}{\alpha 4\pi GM_\odot c} = \frac{L_\odot}{\pi GM_\odot c} \approx 3\text{g/m}^2$ or alternatively $\frac{A}{m} = 327\text{m}^2/\text{kg}$ as the sail area required for a given payload. In other words, if the radial radiation pressure is to carry a 30-ton habitable craft straight out of the solar system, it would require ten square kilometers worth of sail even if we could disregard the mass of the sail itself.

To compare, some of the thinnest commercially used book paper reaches grammages of 25g/m^2 with an $\alpha = 0.06$, while the thinnest materials in consideration for application as solar sails come down to 5.27g/m^2 or $\alpha = 0.29$. If the thickness could be further halved, an enterprising astronaut on their way to Mars could toss a sheet of it out of the solar system as soon as they left Earth's gravity well.

A solar sail-ship capable of adjusting its effective cross-section between sub-critical and critical values will be able to go anywhere beyond Earth in a single orbit. We find that the greatest orbital ratio of two successive planets lies between Mars and Jupiter, at 3.41. To bridge that gap in a single elliptic orbit, a radially aligned solar sail launched from Mars would need either an $\alpha > 0.35$ or some assist letting it exceed Mars' orbital velocity. To reach Mars from Earth, you would only need an $\alpha > 0.17$, which is within our current technological ability.

Of course, a practically engineered solar sail needs not be symmetrically designed or radially aligned, and a slanted reflective sail can provide an orbital acceleration just like the sails of a water-based sailboat can. At non-relativistic speeds this easily overcomes the Poynting-Robertson effect for a reflective surface - though amusingly, if one slants the sail forward only half as much as the Poynting-Robertson slants the sun's rays, the photons will "scoop" to reflect on the front of the sail in a way that provides a *negative* radial force.

The Earth-Mars transfer orbit

When evaluating propulsion methods for individual missions to Mars, one has to consider whether launching a large sail out of Earth's gravity well is more efficient than providing the same thrust to the payload without the sail. If the sail makes up a significant portion of the craft's mass, it may require more energy to lift it out of Earth's gravity well than is necessary to propel the payload alone to Mars.

However, once a sufficiently large sail *is* in space, it would be able to easily carry light cargo back and forth between high-Earth-orbit and Mars without need for further propulsion. This is an ineffective method for rocket-based craft, because any cargo to be loaded near the Earth would need to match the carrier's initial orbital velocity, and so would be able to coast to Mars on its own. On the other hand, a sail surfing on the radial radiation pressure would be able to match much lower loading speeds near the Earth, but its elliptic trajectory could carry small payloads on each trip, making up the energy loss through slants or gravity assists.

The size of the payload would depend on the effective cross-section of the sail, the relative positions of Earth and Mars at that time, and whether one wishes to spend time accelerating the orbital speed through slanting the sail instead of surfing. The latter is a bit of a trade-off, since inclining the sail to increase the relative cross-section β simultaneously decreases the radial cross-section α.

Poynting-Robertson in the Solar system

It should be clear that since planetary orbits appear stable, the Poynting-Robertson effect can't be as dominant as it appears in fig. 4.1. To put things into perspective, let's ask whether the effect of radiation pressure effect on a planet exceeds the decrease in gravitation caused by the energy leaving the sun in the first place.

For the Earth, at orbital radius R with observed solar luminosity W, we get

$$\dot{E}_{\mathbf{grav}} = -\frac{Gm\dot{M}}{R} = \frac{Gm}{R} 4\pi R^2 W = 4\pi RWGm \tag{4.21}$$

$$\dot{E}_{\mathbf{PR}} = -\gamma^3 v^2 WA \approx -\pi r^2 v^2 W \tag{4.22}$$

$$\Rightarrow \frac{|\dot{E}_{\mathbf{grav}}|}{|\dot{E}_{\mathbf{PR}}|} = \frac{4GmR}{v^2 r^2} \approx 4\frac{m}{M}\left(\frac{R}{r}\right)^2 = 6.6 \cdot 10^3 \tag{4.23}$$

In other words, the energy gained from the sun getting lighter as it radiates is three orders of magnitude larger than the energy lost to the Poynting-Robertson effect - and even though the sun loses roughly $4 \cdot 10^9$kg/s, that only corresponds to $6.7 \cdot 10^{-14}\%$ of the total mass per year, and that isn't very noticeable!

Planet	$\frac{\lvert\dot{E}_{\mathbf{grav}}\rvert}{\lvert\dot{E}_{\mathbf{PR}}\rvert}$	Body	$\frac{\lvert\dot{E}_{\mathbf{grav}}\rvert}{\lvert\dot{E}_{\mathbf{PR}}\rvert}$
Mercury	$3.8{\cdot}10^2$	Pluto	$6.6 \cdot 10^5$
Venus	$3.2{\cdot}10^3$	Ceres	$1.4 \cdot 10^3$
Earth	$6.6{\cdot}10^3$	2 Pallas	$1.0 \cdot 10^3$
Mars	$5.8 \cdot 10^3$	4 Vesta	$9.6 \cdot 10^2$
Jupiter	$4.8 \cdot 10^5$	10 Hygiea	$1.2 \cdot 10^3$
Saturn	$7.0 \cdot 10^5$	624 Hektor	$9.8 \cdot 10^2$
Uranus	$2.2 \cdot 10^6$	951 Gaspra	$1.5 \cdot 10^2$
Neptune	$7.0 \cdot 10^6$	25143 Itokawa	$1 \cdot 10^{-1}$

Data source: WolframAlpha Knowledgebase, 2015

Table 4.2: First-order energy ratio estimates assuming a black sphere model.

In table 4.2 we see similar calculations for other objects in the solar system. It's worth disclaiming that for high-albedo asymmetric asteroids this can be orders of magnitude off, but the general trend of smaller objects experiencing a larger relative contribution should still hold.

Chapter 5

The cosmic background fluid

We've seen how radiation affects trajectories through its kinematic pressure near a star. However, radiation is not only found near stars. Even in the interstellar medium, far from any given star, there is a background radiation field. This is not only because of the nearest light sources, for there is an ambient *cosmic background radiation* field of around 2.7 Kelvin, which is believed to be a heat relic of the Big Bang. This chooses a subtly special reference frame in the sense that the cosmic background radiation looks isotropic in it.

Note that this does not violate Einstein's special relativity because it doesn't change the form of any physical laws. Measuring speed relative to the cosmic background radiation is only a slightly more general variant of measuring relative to the Sun or the Earth.

Nevertheless, deviation from this frame has consequences thanks to an isotropic version of the Poynting-Robertson effect. Pressures increase in your direction of travel, draining ever so slight amounts of energy until you come to rest in the fluid. In that sense, the expansion of the universe can be intuited in terms of its effect on the radiation field: as the universe expands, the radiation energy is distributed over a larger area, and even if an object were to not be pulled along by space-time alone, the expanding radiation would provide a source of drag.

On the single-particle scale, a similar argument gives rise to the *Greisen-Zatsepin-Kxuzmin limit*, which puts an upper bound on the energy of ultra-relativistic charged cosmic rays coming from distant sources. However, this is not so much a kinematic effect as it is a quantum one: if a proton has an energy higher than about 8 Joules, the blue-shifted cosmic background photons will be energetic enough to produce π^0-particles through interaction with the proton, thereby transforming kinetic energy into mass in the center-of-energy frame.

The GZK limit seems to correspond well to most observations of cosmic rays, but for a simple extended surface undergoing purely kinetic interaction there is no clear energy cut-off under which the dominant interaction is suppressed. Instead, such a surface smoothly experiences more and more resistance or drag, which is reminiscent of the Poynting-Robertson effect.

This chapter aims to investigate the more general interaction between a relativistic fluid and a surface.

5.1 Relativistic fluids

In general, the stress-energy of a relativistic fluid can be written as

$$T^{\mu\nu} = \underbrace{(\rho + p)U^\mu U^\nu - pg^{\mu\nu}}_{\text{Co-moving terms}} + \underbrace{(U^\mu q^\nu + q^\mu U^\nu) + \pi^{\mu\mu}}_{\text{Transverse terms}} \tag{5.1}$$

where U^μ is a flow vector, ρ is the rest-frame energy density, p is the isotropic pressure, q^μ is a heat flux vector and $\pi^{\mu\nu}$ is a viscous shear tensor. These terms can be grouped into three types:

1. Matter, which in the rest frame appears only in the time component: $\rho U^\mu U^\nu$.

2. Pressure, which in the rest frame is projected onto the spatial components: $p(U^\mu U^\nu - g^{\mu\nu})$.

3. Shear effects, which are orthogonal to the fluid's motion:
   $q^\mu U_\mu = 0$
   $\pi^{\mu\nu} U_\nu = 0$.

The usual treatment of relativistic fluids restricts itself to *perfect fluids*, which are assumed to have no shear components, and so have simplified stress-energy tensors of the form

$$T^{\mu\nu} = (\rho + p)U^\mu U^\nu - pg^{\mu\nu} \tag{5.2}$$

which is fair to use for fluids without significant interaction.[1]

When investigating the evolution of the universe, one commonly further restricts to the two interesting special cases mentioned in section 3.2: Dusts, which for velocities much smaller than the speed of light have negligible pressure and describe a matter-dominated universe, and radiation fluids, which are akin to classical photon gases in that the equation of state is $\rho = 3p$.

While useful tools to describe the various stages of the universe on a large scale, it proves too broad when it comes to describing specific interactions with physically extended objects. Using the stress-energy tensor for a radiation fluid as given, for instance, would imply that a test surface moving along one of its normals through a radiation fluid would experience pressure from the front equal to the pressure from the back, resulting in no net force, when intuitively the Doppler effect would result in a momentum difference of $2\gamma\omega\cos\theta$ between forward- and backward-facing photons at an angle θ with the trajectory.

The reason for the inadequacy is that when a physical object interacts with the stress-energy, it not only affects the object's trajectory, it also changes the stress-energy through shading, reflection, absorption and emission. When we treated the interaction near the Schwarzschild star this was a simple case of choosing what surfaces were in the shade, but in an approximately isotropic background radiation, each part of the surface is only partially shaded.

[1] While photon-photon interactions do occur, implementing it as a shear viscosity for the purposes of matter creation is beyond the scope of this document.

Movement in a radiation fluid

We need to model an ensemble of directed photons, distributed in such a way that they recover the perfect fluid in the absence of an interfering object. In the isotropic CMB frame the velocity distribution of such ambient radiation is simple:

$$U^\mu(\phi,\theta) = (1, -\cos\theta\sin\phi, -\sin\theta\sin\phi, -\cos\phi) \tag{5.3}$$

$$dT^{\mu\nu}(\phi,\theta) = \Phi(\theta,\phi)U^\mu U^\nu d\Omega \tag{5.4}$$

where the coordinate photon density is $\Phi(\theta,\phi)d\Omega = \Phi_0 d\theta d(\cos\phi)$. If we integrate both angles, we get

$$T^{\mu\nu} = \int_{-1}^{1} d(\cos\phi)\int_0^{2\pi} d\theta dT^{\mu\nu} = 4\pi\Phi_0 \mathrm{diag}\left(1,\frac{1}{3},\frac{1}{3},\frac{1}{3}\right) \tag{5.5}$$

which is in accordance with the expression for a radiation fluid in its rest frame. If we only wish to calculate the contributions of the photons relevant to a moving, partially shaded surface, we can transform to a co-moving frame and use the formula for relativistic beaming to determine the integration limits:

$$\cos\phi \mapsto \frac{\cos\alpha - v_z}{1 - v_z\cos\alpha} \Rightarrow 0 \mapsto 0, \frac{\pi}{2} \mapsto \arccos(-v_z), \pi \mapsto \pi \tag{5.6}$$

This allows us to easily calculate the rest-frame force experienced by each surface of an isotropically radiating black cube moving along one of its normals.

$$\begin{aligned} F^\mu_{\mathbf{Front}} &= A(g^\mu_\alpha - u^\mu u_\alpha)\int_{-v_z}^{1} d(\cos\phi)\int_0^{2\pi} d\theta T^{\alpha\nu}n_\nu \\ &= -\frac{2\pi\Phi_0 A}{3}\frac{(1+v_z)^2}{1-v_z}\hat{z}^\mu \end{aligned} \tag{5.7}$$

$$\begin{aligned} F^\mu_{\mathbf{Back}} &= A(g^\mu_\alpha - u^\mu u_\alpha)\int_{-1}^{-v_z} d(\cos\phi)\int_0^{2\pi} d\theta T^{\alpha\nu}n_\nu \\ &= \frac{2\pi\Phi_0 A}{3}\frac{(1-v_z)^2}{1+v_z}\hat{z}^\mu \end{aligned} \tag{5.8}$$

$$\begin{aligned} F^\mu_{\mathbf{Side}} &= A(g^\mu_\alpha - u^\mu u_\alpha)\int_{-1}^{1} d(\cos\phi)\int_0^{\pi} d\theta T^{\alpha\nu}n_\nu \\ &= -\pi\Phi_0 A\gamma v_z\hat{z}^\mu + \frac{2\pi\Phi_0 A}{3}n^\mu \end{aligned} \tag{5.9}$$

The transverse forces on the side cancel due to symmetry, leaving

$$F^z_{\mathbf{Front}} - F^z_{\mathbf{Back}} = -v_z(4\gamma^2-1)T^{33}A \tag{5.10a}$$

$$F^z_{\mathbf{Drag}} = -\gamma v_z T^{00}A \tag{5.10b}$$

$$F^z_{\mathbf{Tot}} = -v_z(4\gamma^2+3\gamma-1)T^{33}A \tag{5.10c}$$

The longitudinal Doppler shift results in both linear and cubic terms, while the total drag force on the sides can be formulated as the Poynting-Robertson effect in its relation to the energy density.

At low speeds, $\gamma \approx 1$ and the drag and frontal forces are approximately equal, the difference being of order $\mathcal{O}(v_z^3)$. This means an isotropically radiating black cube experiences roughly the same force as a reflective cube, but a general black body is less sensitive to asymmetry than a reflective body is. This agrees with the uniform field case, as the reflective surface can steer by sailing transversally.

5.2 A model of shadow

Until now, we've investigated how an object is affected by the presence of a radiation field, but in light of having to include partial shading, we may want to turn the question on its head: how is the radiation field affected by the presence of an object? Using the method of the previous section, we can now model the consequences of a massless black sphere at rest in an isotropic and otherwise homogenous radiation fluid. Realistically, most physical surfaces are coarse enough to radiate its thermal energy chaotically, but in order to differentiate this model from a purely reflective or transparent surface, let's assume a perfect sphere which only radiates radially. This will affect the total stress-energy by replacing the otherwise isotropic radiation shadowed by the object with a radially directed beam.

Resultant stress-energy

Consider a black, radially radiating sphere of radius R at rest. Using the rest-frame integration limits from the previous section we see that an infinitesimal surface element dA absorbs energy at a rate of $T^{0i}n_i dA = \pi\Phi_0 dA$. This translates to radial radiation from that surface element, which decays at a rate of $\frac{R^2}{r^2}$ as the distance r from the origin increases.

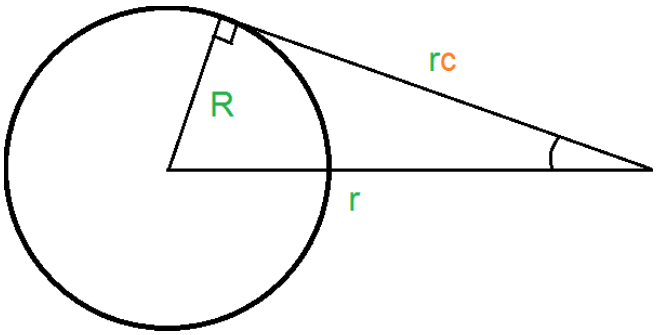

Due to the spherical symmetry we can without loss of generalization consider any point as extending from the sphere's south pole. The azimuthal integration limit for the stress-energy due to the shadow of the sphere is then

$$R = r\sin\phi \Rightarrow \cos\phi = \sqrt{1 - R^2/r^2} \equiv c \tag{5.11}$$

So the total radiation stress-energy $\mathcal{T}^{\mu\nu}$ is calculated to be

$$\begin{aligned}\mathcal{T}^{\mu\nu}(r) &= \int_0^{2\pi} d\theta \int_{-1}^{c} d(\cos\phi) dT^{\mu\nu} + \pi\Phi_0 \frac{R^2}{r^2}\lambda^\mu\lambda^\nu \\ &= \frac{1+c}{2}T^{\mu\nu} + \frac{R^2}{r^2}\frac{\pi\Phi_0}{3}\left(\mathrm{diag}(3, c, c, 3-2c)\right)\end{aligned} \tag{5.12}$$

We see that the Minkowski trace is $\mathcal{T}^{00} - \mathcal{T}^{11} - \mathcal{T}^{22} - \mathcal{T}^{33} = 0$, just as with the general radiation fluid. We also have that as $r \gg R \Rightarrow c \mapsto 1$, which returns to the isotropic stress-energy $T^{\mu\nu}$, while when $r = R$ the radial pressure is 2.5 times larger than the transverse pressure. The lack of off-diagonal terms is because we chose the rest frame for simplicity - in a moving frame the expression can be expected to be far more complicated, with different results depending on whether the sphere is heat-conductive or not.

The gravity of a shadow

We know from the Einstein equation that a change in stress-energy implies a change in the metric, and it's therefore of interest to inquire about the weak gravitational field generated by the mere presence of this shadow. For this we use the linearized field equation (3.23b), which is further simplified by the tracelessness of the stress-energy:

$$\Box h_{\mu\nu} = k\left(\mathcal{T}_{\mu\nu} - \frac{1}{2}\eta_{\mu\nu}T^{\alpha}_{\alpha}\right) \tag{5.13}$$

$$\Rightarrow \Box h_{\mu\nu} = k\mathcal{T}_{\mu\nu} \tag{5.14}$$

Now, any harmonic vacuum solution can be inserted on the left-hand side without affecting the right-hand side. These would be gravitational waves, which are not of interest to a static system such as this. If we can assume our metric independent of time we reduce to the Laplace equation with sources instead:

$$\nabla^2 h_{\mu\nu} = -k\mathcal{T}_{\mu\nu} \tag{5.15}$$

Were it not for discarding the trace, the static weak-field approximation of Newtonian gravity would satisfy this. In fact, the general solution given by

$$h^{\mu\nu}(x) = 4\int d^3x' \frac{\mathcal{T}^{\mu\nu}(x')}{|x - x'|} \tag{5.16}$$

looks quite similar to the Newtonian calculation for the gravitational potential of a source distribution. We briefly despair over the divergence of the infinite contributions in an infinite universe, but then move on and shuffle the divergence into the cosmological constant since we're only interested in the difference relative to the isotropic case which we assume to be flat Minkowski space. In effect this translates to letting $\mathcal{T}^{\mu\nu} \mapsto \mathcal{T}^{\mu\nu} - T^{\mu\nu}$ when it comes to evaluating the integral.

Time metric

Using the spatial symmetry of the energy density, we calculate the contribution from the stress-energy of each spherical shell of radius r to the metric at a point Z away from the origin.

$$\Delta h^{00} = 4 \cdot \int_0^{2\pi} d\theta r^2 dr \mathcal{T}^{00}(r) \int_{-1}^{1} \frac{d\cos\phi}{\sqrt{(Z - r\cos\phi)^2 + r^2\sin^2\phi}} \tag{5.17a}$$

$$= 8\pi r^2 \mathcal{T}^{00}(r) dr \int_{-1}^{1} \frac{d\cos\phi}{\sqrt{Z^2 - 2Zr\cos\phi + r^2}} \tag{5.17b}$$

$$= 8\pi r^2 \mathcal{T}^{00}(r) dr \frac{2}{\max(r, Z)} \tag{5.17c}$$

$$= \frac{16\pi r^2}{\max(r, Z)} \left(\frac{c-1}{2}4 + \frac{R^2}{r^2}\right) \pi\Phi_0 \tag{5.17d}$$

To simplify calculations, we adopt units of $\pi^2\Phi_0$.

$$\begin{aligned}\Rightarrow \Delta h^{00} =& \frac{16r^2}{\max(r,Z)}\left(2c-2+\frac{R^2}{r^2}\right) \\ =& \frac{-16r^2}{\max(r,Z)}(1-c)^2\end{aligned} \tag{5.18}$$

If we integrate this expression directly, we get several levels of divergence. However, if we expand c in terms of $\frac{R^2}{r^2}$, we see that

$$2c = 2\sqrt{1-\frac{R^2}{r^2}} = 2-\frac{R^2}{r^2}-\frac{R^4}{4r^4}-... \tag{5.19}$$

which means that the first two expansion terms are precisely enough to counterbalance the other divergent terms. The exact expression is

$$h^{00} = -16\int_R^Z \frac{r^2}{Z}(1-c)^2dr - 16\int_Z^\infty r(1-c)^2dr \tag{5.20a}$$

$$= \frac{16}{3Z}\left[(2c-2)r^3+(3-2c)R^2r\right]_R^Z + 16\left[(c-1)r^2-\ln(c+1)R^2\right]_Z^\infty \tag{5.20b}$$

$$= \frac{16}{3}\left((1-c)Z^2+(3-2c)R^2-\frac{R^3}{Z}+3R^2\ln\left(\frac{c+1}{2}\right)-\frac{3R^2}{2}\right) \tag{5.20c}$$

$$= \frac{16}{3}\left((1-c)Z^2+\left(\frac{3}{2}-2c+3\ln\left(\frac{c+1}{2}\right)\right)R^2-\frac{R^3}{Z}\right) \tag{5.20d}$$

where c is now evaluated at $r=Z$. We see that the series expansion of c once more presents a cancellation of both divergent and constant terms, so the leading orders are

$$h^{00} \approx \frac{16}{3}\frac{R^3}{Z}+2\frac{R^4}{Z^2}+\frac{1}{6}\frac{R^6}{Z^4}+\mathcal{O}\left(\frac{1}{Z^6}\right) \tag{5.21}$$

The dominant term, which arises from the lowest integration limit at R, can also be written as $\frac{4\pi R^3}{3}T^{00}/Z$, which precisely corresponds to how h^{00} experiences a "hole" of missing energy which fails to attract gravitationally. Of course, if we assume the object to be massive, this term competes with the Newtonian weak static field. Thanks to the linearity of our simplified equations, however, this would not affect the contribution from the traceless part of the stress-energy, which remains a perturbation.

Spatial metric

The spatially indexed elements are a little more complicated, as the contribution of each spherical shell can be split into a symmetric and asymmetric part. The symmetric contributions are almost a third of h^{00}, the only difference appearing in the higher-order terms of $c-1$:

$$\begin{aligned}\Delta h^{ii}_{\mathbf{symm}} =& \frac{16r^2}{3\max(r,Z)}\left(2c-2+c\frac{R^2}{r^2}\right) \\ =& \frac{\Delta h^{00}}{3}+\frac{16R^2dr}{3\max(r,Z)}(c-1)\end{aligned} \tag{5.22}$$

The asymmetric term, which arises from the direction of the beam term $\lambda^\mu\lambda^\nu$, has its Z-contribution from each point on a sphere weighted by the azimuthal angle as $\cos^2\phi$ and the XY-contributions by $\sin^2\phi\sin^2\theta$ and $\sin^2\phi\cos^2\theta$ so the total contribution from such a shell isn't proportional to $(\max(r,Z))^{-1}$ but rather

$$\Delta h^{zz}_{\mathbf{asymm}} = 8R^2\,(1-c)\,dr\int_{-1}^{1}\frac{d(\cos\phi)\cos^2\phi}{\sqrt{Z^2-2Zr\cos\phi+r^2}} \tag{5.23a}$$

$$= \frac{16}{3}R^2\,(1-c)\,dr\cdot\begin{cases}\frac{1}{Z}+\frac{2}{5}\frac{r^2}{Z^3} & Z>r>R\\ \frac{1}{r}+\frac{2}{5}\frac{Z^2}{r^3} & Z<r\end{cases} \tag{5.23b}$$

and

$$\Delta h^{xx}_{\mathbf{asymm}} = 4R^2\,(1-c)\,dr\int_{-1}^{1}\frac{d(\cos\phi)(1-\cos^2\phi)}{\sqrt{Z^2-2Zr\cos\phi+r^2}} \tag{5.24a}$$

$$= \frac{16}{3}R^2\,(1-c)\,dr\cdot\begin{cases}\frac{1}{Z}-\frac{1}{5}\frac{r^2}{Z^3} & Z>r>R\\ \frac{1}{r}-\frac{1}{5}\frac{Z^2}{r^3} & Z<r\end{cases} \tag{5.24b}$$

We see that the first terms exactly cancel the symmetric contribution, and the remainder relates the Z and XY contributions by a relative factor -2, as required by tracelessness. The net contribution of a spherical shell is then

$$\Delta h^{zz} = \frac{\Delta h^{00}}{3}+\frac{32R^2}{15}\,(1-c)\,dr\cdot\begin{cases}\frac{r^2}{Z^3} & Z>r>R\\ \frac{Z^2}{r^3} & Z<r\end{cases} \tag{5.25}$$

$$\begin{aligned}\Rightarrow h^{zz} &= \frac{h^{00}}{3}+\frac{32R^2}{15Z^3}\left[(1-c^3)\frac{x^3}{3}\right]_R^Z+\frac{32Z^2}{15}\left[-\frac{R^2}{2x^2}-\frac{c^3}{3}\right]_Z^\infty\\ &= \frac{h^{00}}{3}+\frac{32}{15}\left((1-c^3)\frac{R^2}{3}-0-\frac{Z^2}{3}+\frac{R^2}{2}+\frac{Z^2c^3}{3}\right) \qquad (5.26)\\ &= \frac{h^{00}}{3}+\frac{16}{9}\left(\frac{2}{5}(c^5-1)Z^2+R^2\right)\end{aligned}$$

$$h^{xx}=h^{yy} = \frac{h^{00}}{3}-\frac{8}{9}\left(\frac{2}{5}(c^5-1)Z^2+R^2\right) \tag{5.27}$$

Once more, if we were to expand $c^5 = 1-\frac{5R^2}{2Z^2}+...$, both divergent and constant terms are cancelled, verifying that it indeed is a weak contribution of leading order Z^{-2}.

$$\begin{aligned}h^{zz} &= \frac{16}{9}\left(\left(\frac{2c^5-5c+3}{5}\right)Z^2+\left(\frac{5}{2}-2c+3\ln\left(\frac{c+1}{2}\right)-\frac{R}{Z}\right)R^2\right) \qquad (5.28)\\ &\approx -\frac{16}{9}\frac{R^3}{Z}+2\frac{R^4}{Z^2}-\frac{1}{6}\frac{R^6}{Z^4}+\mathcal{O}\left(\frac{1}{Z^8}\right)\end{aligned}$$

$$\begin{aligned}h^{xx} &= \frac{16}{9}\left(\left(\frac{6-5c-c^5}{5}\right)Z^2+\left(1-2c+3\ln\left(\frac{c+1}{2}\right)-\frac{R}{Z}\right)R^2\right) \qquad (5.29)\\ &\approx -\frac{16}{9}\frac{R^3}{Z}+\frac{1}{6}\frac{R^6}{Z^4}+\mathcal{O}\left(\frac{1}{Z^6}\right)\end{aligned}$$

While these calculations seem to work out, they're not very pretty. The first thing we can do is define some quantities like the negative vacuum energy

parameter of the missing volume and the quantities in the parantheses that are only dependent on the ratio $\frac{R}{Z}$ through c, using $Z^2 = \frac{R^2}{1-c^2}$:

$$M \equiv \frac{4\pi R^3}{3} \cdot \frac{4\pi \Phi_0}{3} \tag{5.30}$$

$$\Theta \equiv \frac{1}{1+c} + \frac{3}{2} - 2c + 3\ln\left(\frac{1+c}{2}\right) \tag{5.31}$$

$$\sigma \equiv 1 - \frac{2}{5}\left(\frac{1-c^5}{1-c^2}\right) \tag{5.32}$$

$$\Rightarrow h^{\mu\nu} = \left(\frac{M\Theta}{R} - \frac{M}{Z}\right)\mathrm{diag}(3,1,1,1) + \frac{M\sigma}{2R}\mathrm{diag}(0,-1,-1,2) \tag{5.33}$$

which we now can rotate to an arbitrary direction to use Z as a radius.

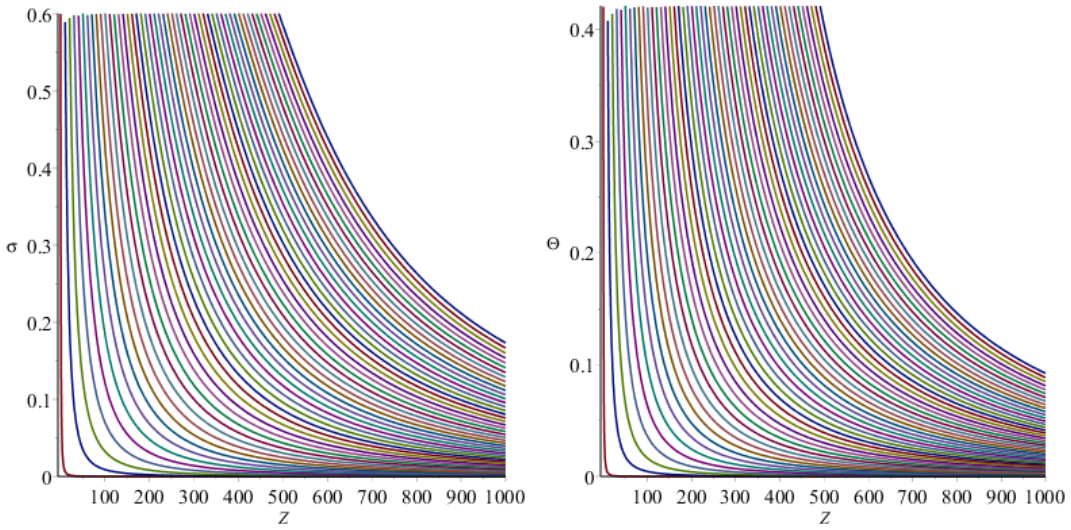

Figure 5.1: σ and Θ for various values of R. As expected, they decay rapidly.

Thus we see that even the slightest correction to homogeneity can have complex consequences for the curvature of space, highlighting how deep the rabbit hole goes. Though we started with something as seemingly straight-forward as the Poynting-Robertson effect, we now see that an object that interacts with photons will implicitly also affect curvature - even if it is at rest! A dynamic shadow such as that arising from the Poynting-Robertson effect would be even more complex, depending on parameters such as the mass, velocity and heat conductivity of the object.

Granted, it's a negligible effect for macroscopic considerations in the real world, but nevertheless an interesting perspective on how chaotic curvature in a radiation-dominated universe must be on the small scale.

Chapter 6

Conclusion and considerations

In chapter 1 we described how we expect a change of reference frame to be able to incur velocity-dependent forces, and promised to investigate the mathematical tools needed to describe such effects in a general setting.

After introducing geodesics, covariant derivatives and four-forces, we've now demonstrated how the Poynting-Robertson effect can be included in dynamic calculations as a non-gravitational term. The parameters relevant to the force were identified, and their meager values for many real-world scenarios explain why the phenomenon is often paid little heed. Though higher-order thermal effects such as the Yarkovsky and YORP effects were identified, they were not treated in as much detail as Poynting-Robertson, which we expect to dominate.

On the way, we acquired a perspective on the viability of solar sails for space travel. While not necessarily the best solution for every situation, it shows clear potential for certain types of missions and is worth further development. In particular, a simulation of the Mars-Earth transfer orbit could see potential application in the future.

Unfortunately, one of the questions asked in the introduction was only given a cursory treatment: Can the metric itself emulate viscosity?

We've seen how the linearized field equations can give rise to implicitly velocity-dependent T^{0i} and by extension g^{0i}-components of the metrics, which is where we would expect the viscous effects to appear. We've also seen how to calculate change in metric arising from a fluid-interacting object, but we only went into detail for the isotropic rest frame as a static contribution. As a future project it would be interesting to augment the shadow model by making the object move, thereby incurring a velocity-dependent effect on the metric both through its own energy-momentum and its fluid-interaction. The question is then whether this procedure could provide the proper friction-like correction to the geodesics through Christoffel symbols rather than as a four-force.

Ultimately we could compare this to the corrections of a weakly Kerr metric to see whether gravitomagnetic frame-dragging can be modelled as a Poynting-Robertson effect based on gravitational radiation. After all, frame-dragging is linear in the orbital velocity, much like the Poynting-Robertson effect for an absorbing body is. The settings may be different, but the similarities spark curiosity.

Bibliography

[1] Hartle, J.B. "Gravity: An Introduction to Einstein's General Relativity" (Addison-Wesley, 2002)

[2] Guess, A.W. "Poynting-Robertson effect for a spherical source of radiation." Astrophysical Journal, vol. 135, p. 855-866 (1962)
http://adsabs.harvard.edu/abs/1962ApJ...135..855G

[3] Poynting, J.H. "Radiation in the solar system: its effect on temperature and its pressure on small bodies". Monthly Notices of the Royal Astronomical Society (Royal Astronomical Society, 1903)
http://rsta.royalsocietypublishing.org/content/roypta/202/346-358/525.full.pdf

[4] Robertson, H.P. "Dynamical effects of radiation in the solar system". Monthly Notices of the Royal Astronomical Society (Royal Astronomical Society, 1937)
http://mnras.oxfordjournals.org/content/97/6/423

[5] Breiter, S. and Vokrouhlicky, D. "YORP effect with anisotropic radiation"
http://arxiv.org/abs/1009.1525v1

[6] Spoto et al. "Non-gravitational Perturbations and Virtual Impactors: the case of asteroid 2009 FD" (2014)
http://arxiv.org/abs/1408.0736

[7] Dundas, B.I. "Differential Topology"
http://folk.uib.no/nmabd/dt/dt.pdf

[8] Kachelriess, M. Lecture notes, "Linearized gravity and gravitational waves."
http://web.phys.ntnu.no/∼mika/grav_part6.pdf